Thesis

Role of neutrophil extracellular trap formation in liver cirrhosis and sarcopenia

submitted by

Manuel Stelzer

in partial fulfillment of the requirements for the degree of

Doktor der gesamten Heilkunde

(Dr. med. univ.)

at the

Medical University of Graz

executed at the

University departments of Internal Medicine

Division of Gastroenterology and Hepatology

under the supervision of

Assoz. Prof.in Priv.-Doz.in Dr.in med. univ. Vanessa Stadlbauer-Köllner,

Irina Balazs, MD, PhD

Graz, 16.11.2023

Declaration of Academic Integrity

I hereby confirm that the present diploma thesis is the result of my own independent scholarly work. I also confirm that in all cases, where material from the work of others (in books, articles, essays, dissertations, and on the internet) is acknowledged, quotations and paraphrases are clearly indicated. No material other than that cited in the reference list has been used. I have read and understood the Medical University's regulations and procedures concerning plagiarism.

Graz, 16.11.2023 *Manuel Stelzer e.h.*

Acknowledgements

Words cannot adequately express my gratitude to my supervisors, Assoz. Prof.in Priv.-Doz.in Dr.in med. univ. Vanessa Stadlbauer-Köllner and Irina Balazs, MD, PhD, for their invaluable support and patience during my thesis. Without their guidance and professional feedback, I would never be able to complete this study successfully. They have totally integrated me into their team since day one and introduced me to science. At this point, I would like to extend my sincere gratitude to Irina Balazs, who spent numerous hours in discussions with me and tirelessly motivated and helped me.

Special thanks to my mother, Sabine, who always believed in me and gave me the opportunity to study medicine. Many thanks to my sister Julia, who supported me throughout my journey. Last but not least, a special thanks to my partner, Lisa Maria, who helped me through difficult moments by encouraging me.

Thank you all!

Zusammenfassung

Hintergrund: Sarkopenie ist eine häufige Komplikation von Patient*innen mit Leberzirrhose, kann aber auch als eigenständige Erkrankung auftreten. Das Immunsystem spielt sowohl bei Leberzirrhose als auch bei Sarkopenie eine wichtige Rolle in der Pathogenese. Die Bildung von neutrophilen extrazellulären Fallen (NETs) wurde bereits mit chronischen Entzündungen in Verbindung gebracht und ihre Funktion kann bei Leberzirrhose verändert sein. Bei Patient*innen mit Sarkopenie wurde dies noch nicht untersucht. Diese Studie zielt darauf ab, herauszufinden, ob die Formation von NETs bei Patient*innen mit Sarkopenie und Leberzirrhose verändert ist.

Methode: Neutrophile Granulozyten von 121 Patient*innen wurden isoliert und mit hitzeinaktivierten *E. coli* (250 Bakterien/Zelle), Phorbol-12-Myristat-13-Acetat (PMA) (100 nM) oder Inkubationsmedium in Duplikaten für 2 Stunden bei 37°C stimuliert. Die Zellen wurden mit Paraformaldehyd fixiert und mit 4′,6-Diamidino-2-phenylindol (DAPI) angefärbt. Bilder von 10 zufälligen Sichtfeldern pro Objektträger wurden mit dem Fluoreszenzmikroskop Olympus BX51 bei 600-facher Gesamtvergrößerung aufgenommen. Der DNA-Area and NETosis-Analysis (DANA) Algorithmus wurde verwendet, um den Prozentsatz der Formation von NETs pro Patient*in zu quantifizieren.

Ergebnisse: Der DANA-Algorithmus wurde erfolgreich optimiert und validiert. Durch den Einsatz von DANA verringerte sich die durchschnittliche Zeit für die Analyse der Formation von NETs von 30 Minuten pro Patient*in (bei konventioneller Augenzählung) auf 5 Minuten (bei Einsatz von DANA; p=0.006). Bei der *ex vivo* Stimulation von Neutrophilen mit *E. coli* (p=0.778) oder mit PMA (p=0.490) wurde zwischen den drei Gruppen kein signifikanter Unterschied in der Formation von NETs beobachtet. Es gab jedoch eine Tendenz zu einer erhöhten Formation dieser bei nicht stimulierten Neutrophilen in der Sarkopenie-Gruppe (p=0.056).

Schlussfolgerung: Auf künstlicher Intelligenz basierende Ansätze können für eine standardisierte und effiziente Analyse der Formation von NETs verwendet werden und

ermöglichen die Analyse für groß angelegte klinische Studien und der routinemäßigen Laboranalyse in klinischer Praxis. Die spontane Formation von NETs war in dieser Studie bei Patient*innen mit Sarkopenie im Vergleich zu Patient*innen mit Leberzirrhose und Leberzirrhose sowie Sarkopenie tendenziell erhöht. Obwohl dies keine statistische Signifikanz erreichte und in weiteren Studien validiert werden muss, ist er der erste Ansatz dafür, dass die Bildung von NETs ein potenzieller Biomarker für Sarkopenie sein und eine Rolle bei ihrer Pathogenese spielen könnte.

Abstract

Background: Sarcopenia is a frequent complication of liver cirrhosis (LC), but it can also occur independently of any underlying cause. The immune system plays an important role in the pathogenesis of both LC and sarcopenia. Neutrophil extracellular traps (NETs) formation has been linked to chronic inflammation, and their function can be altered in people with LC; however, NETs formation in patients with sarcopenia has not been studied yet. Here, we aimed to study if NETs formation is altered in patients with sarcopenia and LC.

Method: Neutrophil granulocytes from 121 patients were isolated and stimulated with heat-inactivated *E. coli* (250 bacteria/cell), phorbol 12-myristate 13-acetate (PMA) (100 nM), or incubation medium in duplicates for 2 hours at 37°C. Cells were fixed with paraformaldehyde and stained with 4′,6-diamidino-2-phenylindole (DAPI). Pictures of 10 random fields of vision per slide were taken with an Olympus BX51 Fluorescence Microscope at 600x total magnification. DNA area and NETosis analysis (DANA) algorithm was used to quantify the percentage of NETs formation per patient.

Results: The DANA algorithm was successfully optimized and validated. The use of DANA decreased mean NETs formation analysis time from 30 minutes per patient (if conventional counting by eye is used) to 5 minutes (if DANA is used; p=0.006). There was no significant difference in NETs formation observed between the three groups of patients upon *ex vivo* stimulation of neutrophils with *E. coli* (p=0.778) or with PMA (p=0.490), but there was a tendency toward increased spontaneous NETs formation in the sarcopenia group (p=0.056).

Conclusion: Artificial intelligence (AI) based approaches can be used for standardized and efficient analysis of NETs formation, making it feasible to introduce NETs formation analysis for large-scale clinical studies and as part of routine lab analysis in clinical practice. Spontaneous NETs formation within this study tended to be increased in patients

with sarcopenia compared to patients with LC and LC + S. Though this finding did not reach statistical significance and has to be validated in further studies, it is the first evidence that NETs formation might be a potential biomarker of sarcopenia and might play a role in its pathogenesis.

List of contents

Abbreviations

ACLF *acute-on-chronic liver failure*

AI *artificial intelligence*

CAID *cirrhosis-associated immune dysfunction*

cfDNA *cell free DNA*

DAMPs *damage-associated molecular patterns*

DANA *DNA Area and NETosis Analysis*

DAPI *4',6-diamidino-2-phenylindole*

DNA *deoxyribonucleic acid*

DNase *deoxyribonuclease*

EWGSOP *European Working Group on Sarcopenia in Older People*

EWGSOP2 *European Working Group on Sarcopenia in Older People 2*

H3Cit *citrullinated histone H3*

HCC *hepatocellular carcinoma*

LC *Liver cirrhosis*, *liver cirrhosis*

LC+S *Liver cirrhosis + sarcopenia*

MPO *myeloperoxidase*

NADPH *nicotinamide adenine dinucleotide phosphate*

NE *neutrophil elastase*

NETs *neutrophil extracellular traps*

PAD4 *protein-arginine deiminase type 4*

PAMPs *pathogen-associated molecular patterns*

PI3K *phosphoinositide 3-kinase*

PMA *phorbol 12-myristate 13-acetate*

ROI *region of interest*

ROS *reactive oxygen species*

SBP *spontaneous bacterial peritonitis*

Figures

Tables

1 Introduction

1.1 Sarcopenia

Sarcopenia is a progressive and generalized skeletal muscle disorder involving the accelerated loss of muscle mass and function associated with increased adverse outcomes, including falls, functional decline, frailty, and mortality (1). It also increases the risk of fractures, impairs the ability to perform activities of daily living, and is associated with cardiac and respiratory diseases, cognitive impairment, lower quality of life, loss of independence, and the need for long-term care placement (2). The term “sarcopenia” was first used in the 1980s by Rosenberg (3) to describe age-related decline in lean body mass. The word was derived from the Greek words “sarx” for flesh and “penia” for loss to express the body composition and function change.

Two milestones have been authoritative for today’s perspective on sarcopenia. The first was the addition of muscle function into several consensus definitions (1). The European Working Group on Sarcopenia in Older People (EWGSOP), for instance, used low muscle mass plus low muscle function (strength and performance) to diagnose sarcopenia instead of the former definitions based only on muscle mass alone (2, 4). The severity of sarcopenia was classified into pre-sarcopenia, sarcopenia, and severe sarcopenia, depending on the presence of these diagnostic criteria (4). Intensive research found that low muscle strength better predicted adverse outcomes than low muscle mass. The European Working Group on Sarcopenia in Older People 2 (EWGSOP2) later adapted the criteria for sarcopenia based on these findings. Low muscle strength, low muscle mass or quality, and low physical performance were then considered in diagnosing sarcopenia (2). The second milestone was the inclusion of sarcopenia into the International Classification of Diseases-10 code (1, 5).

There has been a growing awareness of sarcopenic obesity due to the rising prevalence of obese patients, a situation in which obesity coexists with diminished muscle mass and function. The conventional definition of this condition has not yet been entirely established. However, evidence suggests it may cause frailty, disability, morbidity, and death. (6).

1.1.1 Causes of sarcopenia

Former views considered sarcopenia a muscle condition in people of older age, but now it is recognized to begin earlier in life (2). Sarcopenia can occur in various diseases or result from many underlying living conditions. For instance, it can be a consequence of nutritional imbalances like low protein or energy intake, micronutrient deficiencies, malabsorption, other gastrointestinal conditions, and anorexia. Sarcopenia can also be associated with physical inactivity, including bed rest, immobility, deconditioning, and a sedentary lifestyle. The most frequent underlying diseases are bone and joint diseases, cardiorespiratory disorders (i.e., chronic heart failure and obstructive pulmonary disease), metabolic diseases (i.e., diabetes), endocrine diseases (i.e., androgen deprivation), neurological disorders, cancer, and liver and kidney disease, as well as iatrogenic nature through hospital admission or drug-related sarcopenia (1). If no underlying cause is identified other than age, sarcopenia is described as primary, while with an evident cause, it is classified as secondary. Since aging can cause many problems in the body concurrently, there can be more than one cause simultaneously (2).

1.1.2 Epidemiology of sarcopenia

The prevalence of sarcopenia is 5-10% among people 65 or older (5), increasing to 11-50% among people 80 and older (7). Nonetheless, the disparity in the prevalence of sarcopenia is based on a lack of exact cutoffs for diagnosis (8). The prevalence also depends on the considered setting: patients in post-acute care settings, care homes, and hospitals are more likely to suffer from sarcopenia than those in the community (1).

1.1.3 Pathophysiology of sarcopenia

The pathophysiology of aging in skeletal muscles is a multifactorial process including many factors like impaired satellite cells, changes in hormones and growth factors, oxidative stress, neural changes and motor neuron loss, mitochondrial dysfunction, inactivity, an imbalance in protein metabolism, inflammation, microvascular changes, and apoptosis (1).

Age-related loss of muscle tissue is characterized by a decreased number and size of myofibers, especially type 2 fibers, leading to decreased strength. Additionally, there is a higher presence of adipose and fibrotic tissue in sarcopenic muscles and fewer satellite cells important for skeletal muscle mass maintenance (9). There is evidence that mitochondrial physiology in muscle cells is altered due to complex pathophysiological pathways affecting reactive oxygen species (ROS) production, promoting inflammation, and leading to cumulative muscle damage (7). This imbalance of ROS in myofibers leads to muscle atrophy in primary sarcopenia (9), promoting inflammation while disrupting skeletal muscle (7).

Previously, sarcopenia was potentially linked to inflammaging, denoting a low-grade chronic systemic pro-inflammatory state with age due to immune system impairment (7). This chronic inflammation is suggested to contribute to age-related sarcopenia. It was found that patients with sarcopenia have increased proinflammatory cytokine levels (i.e., Interleukin-6 and, C-reactive protein), while recently, anti-inflammatory cytokines (Interleukin-4 and Interleukin-10) have been shown to retard sarcopenia and alleviate muscle atrophy. In sarcopenic obesity, fat infiltration is also recognized as a condition with increased local inflammation due to proinflammatory cytokines and adipokines like leptin and adiponectin produced by adipocytes associated with sarcopenia development (7).

1.2 Liver cirrhosis

Liver cirrhosis (LC) is a multi-systemic disease where healthy liver parenchyma is chronically replaced by fibrotic tissue due to persistent inflammation (10, 11). Histologically, the permanent liver injury rebuilds tissue into regenerative nodules surrounded by fibrous bands composed of collagen, further leading to abnormal hepatocyte function, vasculature, and blood flow (12). LC is associated with high morbidity and mortality, causing more than 1.32 million (2.4% of all) deaths worldwide in 2017. Thus, it was the 13th-leading cause of death. The main causes of LC worldwide are related to chronic alcohol abuse, obesity, and viral hepatitis B and C (10, 11, 13, 14). Other causes include overloading the liver with iron or copper, alpha1-antitrypsin deficiency, autoimmune hepatitis, or drug-related cirrhosis. The disease can even progress faster if more cirrhotic risk factors are coincident (11).

1.2.1 Classification of liver cirrhosis

The LC stage depends on the stage of liver fibrosis and the presence of clinical symptoms of the disease. Commonly, LC is defined by stage 4 liver tissue fibrosis. LC is recognized as being in the asymptomatic phase if there are no further complications other than fibrosis. The onset of complications related to LC usually defines the decompensated phase. If the disease progresses, it can lead to acute-on-chronic liver failure (ACLF) with either hepatic or extrahepatic organ failure. There is no consensus on whether ACLF is a syndrome or a terminal stage, but independently of its definition, it has the highest short-term mortality among people with LC. Generally, mortality risk increases with each stage (i.e., compensated, decompensated, and ACLF) as well as comorbidities (i.e., cardiovascular disease, malignancy, diabetes, sarcopenia, and frailty) and underlying causes (10).

1.2.2 Complications of liver cirrhosis

The progression of cirrhosis affects portal blood resistance and can lead to portal hypertension, further leading to ascites, hepatorenal syndrome, gastro-esophageal varices, and hepatic encephalopathy. Liver dysfunction can further lead to non-obstructive jaundice and portal vein thrombosis. Patients with LC are susceptible to bacterial infections, which can trigger organ failure and ACLF. Bacterial infections highly worsen the prognosis of patients with LC and increase the probability of mortality by four times. Especially spontaneous bacterial peritonitis (SBP) and urinary tract infections are present in these patients. Additional complications regarding the physical condition of these patients are malnutrition, frailty, and sarcopenia, occurring parallel to the severity of cirrhosis.

Whereas patients with compensated LC die of renal disease, malignancy, or cardiovascular disease, in decompensated LC, the leading causes of death are consequences of portal hypertension and hepatocellular carcinoma (HCC) (10).

1.3 Liver cirrhosis and sarcopenia

In general, the prevalence of sarcopenia in liver disease ranges from 30-70% depending on the study (15), and the overall prevalence in general is about one-third of people suffering from cirrhosis. Nevertheless, it is higher in men. (16). The prevalence increases in patients with alcohol-related liver disease and a greater severity of cirrhosis. According to mortality and survival, sarcopenia is highly and independently associated with a higher risk of death and a lower probability of surviving in 1-, 3-, and 5-year survivals. Hence, patients with sarcopenia and LC generally have an approximately two-fold higher risk of death than those without it (16). Therefore, further research should be prioritized to develop therapeutic and preventive approaches for muscle loss in liver disease.

The main driver of sarcopenia in LC is an imbalance between protein synthesis and catabolism. The main mechanisms leading to sarcopenia in cirrhosis are linked to myostatin, which indirectly activates autophagy and the ubiquitin-proteasome pathway. Another pathway involves rapamycin (mTOR). Moreover, hyperammonemia highly influences muscle physiology. There is evidence that sarcopenia is not limited to skeletal muscle but also affects cardiac muscle and the diaphragm, contributing to cardiac and respiratory dysfunction (17).

1.4 Liver cirrhosis, sarcopenia, and immune dysfunction

A recently upcoming view describes that chronic replacement of liver parenchyma by fibrotic tissue is additionally caused by local and systemic inflammation that occurs due to immune alterations, especially innate immunity (11). LC has been associated with immune dysfunction, so-called cirrhosis-associated immune dysfunction (CAID), subsuming systemic inflammation and immune deficiency. The intensity of immune alterations depends on the stage of LC and culminates in ACLF. There is a low-grade systemic inflammatory phenotype, usually in compensated or decompensated liver disease without organ failure, and a high-grade systemic inflammatory phenotype in ACLF. Immunodeficiency in LC can be explained by impaired immune system function, where immune cells' function is altered along with structural distortion of the liver. Hepatocyte loss reduces immune protein synthesis, reducing immune system activation while leading

to increased susceptibility to infection and less immunity to microorganisms entering the body through the portal vein.

Neutrophils play a critical role in the innate immune response. Neutrophils are depleted due to splenic sequestration, have impaired phagocytic activity, and have reduced chemotaxis to the site of infection in patients with LC. Furthermore, they have an elevated basal ROS release, which can contribute to tissue damage and fibrosis and lead to neutrophil functional exhaustion in patients with LC (18). Additionally, degranulation and bacterial killing become insufficient (11). Notably, neutrophil dysfunction and immunodeficiency generally result in increased susceptibility to bacterial infections, and mortality even in compensated LC.

Systemic inflammation is mainly driven by dysbiosis and intestinal barrier disruption with increased permeability in LC, contributing to additional immune system stimulation by pathogen-associated molecular patterns (PAMPs). Under non-infectious conditions, damage-associated molecular patterns (DAMPs) can activate the immune system. These PAMPs and DAMPs bind to specific receptors, increasing inflammatory cytokines and immune effector cells and leading to systemic inflammation. (18). Not much is known concerning the association between innate immunity and sarcopenia. The dysregulation of neutrophil chemotaxis in older age may play a key role in secondary systemic inflammation (8). Neutrophils migrate with less accuracy, which potentially causes increased collateral damage. The underlying mechanism may be dysregulated phosphoinositide 3-kinase (PI3K) activity (19). This collateral damage may cause loss of muscle function; therefore, therapeutic strategies targeting the PI3K pathway can potentially restore neutrophil chemotaxis (8, 19).

1.5 Neutrophil granulocytes

Neutrophil granulocytes are the most abundant leukocytes in human blood as part of the innate immune system (20). They protect the human body against bacteria and fungi and help defend organisms from parasites and viruses. Before operational, neutrophils undergo complex differentiation steps from hematopoietic stem cells in bone marrow to mature neutrophil granulocytes, requiring over 10 days. Approximately 1 billion neutrophils per

kilogram of body weight are produced daily, increasing up to 10 billion during infections (21). Once in blood circulation, their half-life ranges from 8 to 20 hours (22). However, after migration into tissues, their life span can extend to 7 days in an inflammatory milieu (21).

Normally, neutrophils circulate in the blood in human vessels. If there is an infection or inflammation, the endothelium in this area is activated, and neutrophils respond by using their receptors to interact with it and roll on the endothelium surface until firm adhesion is achieved by several adhesion receptors and tethers as well as slings (21). Neutrophils also react to damage signals without infection. Activation receptors are generally known as pattern recognition receptors (22). Fully coherent neutrophils transmigrate through the endothelium and basal membrane, arrive in the interstitial space, and follow chemotactic gradients to their initial target. There they eliminate the pathogen using phagocytosis, exocytosis by releasing proteases and ROS, and by forming extracellular traps. Thus, they release mediators for further response in the innate and adaptive immune systems (21).

Neutrophils store intracellular granules that can be rapidly used to sufficiently protect against pathogens. For instance, the release of granule content can be primed by PAMPs. The disadvantage of these granules is that their substances also cause tissue damage. For example, uncontrolled release of proteolytic enzymes is associated with metabolic syndrome, fibrosis, systemic inflammatory response syndrome, sepsis, physical trauma, and cancer progression (21).

1.6 Neutrophil extracellular traps

Neutrophil extracellular traps (NETs) were first discovered in 2004 (23). Since then, scientific interest has grown but is far from fully understanding NETs biology in health and disease. NETs are known to capture, neutralize, and eliminate bacteria (23), fungi (24), viruses (25), and even parasites (26). However, their potentially toxic enzymes can otherwise induce massive tissue damage and contribute to disease.

NETs are web-like structures composed of cytosolic and granule proteins on decondensed chromatin fibers. These structures are formed by deoxyribonucleic acid (DNA) from the nucleus (20) but also consist of mitochondrial DNA (27, 28). Although the dominant

proteins are histones, neutrophil elastase (NE), and myeloperoxidase (MPO), there are up to 50 proteins involved depending on the stimulus (20).

The process of NETs formation was initially seen as a cell death mechanism called NETosis (29). Later, it was found that a non-lytic NETosis variant without cell death existed (27, 28). In contrast to slowly occurring NETosis, the non-lytic process is characterized by a rapid release of NETs without dying afterward.

MPO, NE, ROS production, and protein-arginine deiminase type 4 (PAD4) have crucial roles in the molecular mechanism of NETs formation. If ROS increases through nicotinamide adenine dinucleotide phosphate (NADPH) oxidase, MPO is triggered, leading to MPO-mediated activation of NE, which inhibits the phagocytosis process while further proteolytically processing histones and disrupting chromatin. Decompensation of chromatin is also influenced by MPO and PAD4, which citrullinate histones. Recently, other pathways of NETs formation independent of NADPH oxidase and ROS production and pathways depending on mitochondrial ROS production have been found. Triggers for these pathways are likely diverse PAMPs and DAMPs, immune complexes, cholesterol crystals, bicarbonate crystals, calcium crystals, and activated platelets. Alternative potential pathways have also been suggested, emphasizing further insights in the future.

Considering the regulation of NETs structures, the microorganism's size seems to be an essential factor. If pathogens are too large to be phagocytosed, NETs pathways are activated(20). If NETs are inhibited, an increased susceptibility to bacterial infection in mice and humans is seen (30). Some pathogens express deoxyribonuclease (DNase) to protect themselves from NETs elimination (31).

Generally, NETs can be visualized *in vitro* using fluorescent, flow cytometry, or electron microscopy (including transmission electron and scanning electron microscopy). Additionally, since NETs consist of DNA, visualization can be expanded by immunostaining using antibodies against DNA components (32), such as MPO-DNA, cell-free DNA (cfDNA), and citrullinated histone H3 (H3Cit). The limitations are that cfDNA can be unspecifically released by any type of cell damage, and MPO-DNA can increase if neutrophils are activated in the absence of NETs formation. Therefore, citrullinated histones like H3Cit are considered more specific (33) since PAD4 catalyzes the citrullination of histones and modifies chromatin (34). Similar techniques and live-cell

imaging methods have been used to further investigate NETs *in vivo* (32). However, since only about 25% of neutrophils release non-lytic NETs, it has been difficult to study NETs formation *in vivo* (30, 35).

To quantify visualized NETs, various methods, including semiautomated and automated approaches, have been developed. Common techniques have included counting by eye, ImageJ and other software, a fluorescent reader, flow cytometry, transmission electron microscopy, and scanning electron microscopy. Parameters like NETs formation percentage, NETs degradation level, DNA release (µg/mL), morphology of NETs-releasing cells, and the amount and structure of NETs-releasing cells have been investigated and compared (32).

1.7 Liver cirrhosis, sarcopenia, and neutrophil extracellular traps

So far, little data is available regarding the role of NETs formation in patients with LC. An *ex vivo* experiment showed decreased NETs formation in patients with alcohol-related liver disease compared to healthy ones. Preclinical models have also shown decreased hepatic NETs formation as well as neutrophil clearance by macrophages (18).

One research group showed that the release of NETs decreased with the decompensation of LC, comparing compensated and decompensated LC (36). The same group investigated NETs from peripheral blood and ascites fluid of patients with SBP compared to NETs from peripheral blood in a healthy group. There, the NETs release was diminished in patients with LC (37).

In contrast, two studies showed increased NETs marker MPO-DNA in patients with LC compared to healthy controls (38, 33). In addition, H3Cit-DNA elevation correlated with the degree of liver dysfunction classified by the Child-Pugh Score. The presence of HCC did not further increase H3Cit-DNA plasma levels (33). Another study group showed higher MPO-DNA as a NETs marker *in vitro* in patients with HCC, especially those with metastasis (39).

It was shown that patients with non-alcoholic steatohepatitis had increased serum levels of MPO-DNA compared to people with normal liver histology. Furthermore, when NETs formation was blocked through DNase or PAD4 inhibition, HCC growth was effectively

reduced in mice, probably due to a reduced inflammation environment. The inflammation reduction was assumed by the lower presence of infiltrating macrophages and the reduced production of inflammatory cytokines (40). However, to our knowledge, NETs formation in sarcopenia has not been studied yet, and the role of NETs formation in LC has been barely described.

1.8 Aim of this study

The aim of this study was to study NETs formation in patients with LC and sarcopenia. Furthermore, we wanted to optimize and implement a published method, DNA area and NETosis analysis (DANA), to quantify the percentage of NETs formation in 4′,6-diamidino-2-phenylindole (DAPI) stained neutrophils in a standardized and fast way.

2 Materials and Methods

2.1 Human samples

Patients with a clinical/radiological/histological diagnosis of cirrhosis hospitalized for any reason were recruited at the Medical University of Graz at the Department of Gastroenterology and Hepatology as part of the study NCT03080129 (ethic vote number: 29-280 ex 16/17). Patients provided written informed consent, and the study was approved by the Medical University of Graz Institutional Review Board and carried out according to the Declaration of Helsinki. Hepatic encephalopathy > grade 2 and/or other cognitive disorders not allowing informed consent, advanced HCC, and age under 18 were exclusion criteria. Sarcopenia was diagnosed according to the EWGSOP 2010 criteria. This part was performed by colleagues prior to the start of my diploma project.

2.2 NETs assay

Peripheral venous blood was taken from 121 patients. Neutrophils were isolated from the blood with Polymorphprep (Axis-shield, Oslo, Norway). Then the neutrophils were stimulated with either phorbol 12-myristate 13-acetate (PMA, 100 nM), heat-inactivated *E. coli* (250 bacteria/cell) or with the incubation medium for two hours at 37°C. After that, cells were fixed with paraformaldehyde and stained with DAPI (Life Technologies, Carlsbad, CA, USA). Pictures of ten random fields of vision were taken with an Olympus BX51 Fluorescence Microscope (Olympus, Shinjuku, Tokyo, Japan) at 600x total magnification per duplicate. This part was performed by colleagues prior to the start of my diploma project. To quantify the percentage of NETs formation for each patient, a DANA workflow was used (41).

2.3 DNA area and NETosis analysis (DANA)

DANA is a semiautomated, high-throughput method to quantify NETs in fluorescent microscope images based on an ImageJ/Java algorithm. All instructions and materials needed to install and run DANA were found on the ShelefLab website. Java version 1.4.0

or later and Fiji, a distribution of the open-source software ImageJ, were used for the analysis.

The DANA algorithm is separated into two parts. The first part is performed in ImageJ/Fiji to quantify the area, raw integrated density, aspect ratio, roundness, maximum and minimum brightness, and solidity of each region of interest (ROI) for each image. One ROI should contain a single cell. The information is then saved in an individual Microsoft Excel csv-file and stored in a defined output folder. For DANA_I, there are two different plugins available. One analyzes the selected picture, and another batch plugin allows you to rapidly analyze all pictures from a selected folder.

Then DANA_II, the second part of DANA, operates in Java and imports all csv-files automatically from the chosen folder. DANA_II calculates the percentage of NETs formation per patient using the parameters from DANA_I and stores the information in a Microsoft Excel csv-file for each image individually, as well as one summary with the average percentage of NETs formation and DNA area for this whole sample. In these files, information about the area, relative area compared to condensed nuclei, NETs status for each ROI, number of NETs, percentage of NETosis, and average cellular DNA for the image are stored. During this process, DANA_II eliminates ROIs, which are suggested as cell fragments or multiples, by comparing their raw integrated densities with the adapted standardized cutoffs. After elimination, the ROIs are then calculated relative to the areas of the five smallest ROIs, which are seen as neutrophils with condensed nuclei.

2.4 Data analysis

IBM SPSS Statistics 27 and GraphPad PRISM 9 were used for statistical analysis. All graphs were created with GraphPad PRISM 9. The Shapiro-Wilk test and histogram were applied to assess the distribution of each group and each condition. A Kruskal-Wallis test was performed on independent samples to find differences in the percentage of NETs formation between the three study groups for each condition (incubation medium, *E. coli*, PMA). Dunn's test was used for post-hoc analysis. A Bland-Altman test and paired t-test were performed to optimize and validate the DANA approach. An unpaired t-test with

Welch´s correction was used to compare analysis time. For all statistical tests, p values less than 0.05 were considered significant.

3 Results

3.1 DANA optimization and validation

DANA was chosen because it has decisive advantages for analyzing fluorescent microscope images. First, it was simple to install, and it does not require any advanced programming skills. It also uses single-channel staining of neutrophils with DAPI and can be optimized for different images as well (Figure 1). Quantifications of the percentage of NETs formation via analyzing microscope images by eye are usually laborious and time-consuming, but the DANA algorithm allows very fast quantifications. The required software, ImageJ and Java, as well as the optimization instructions, are freely available.

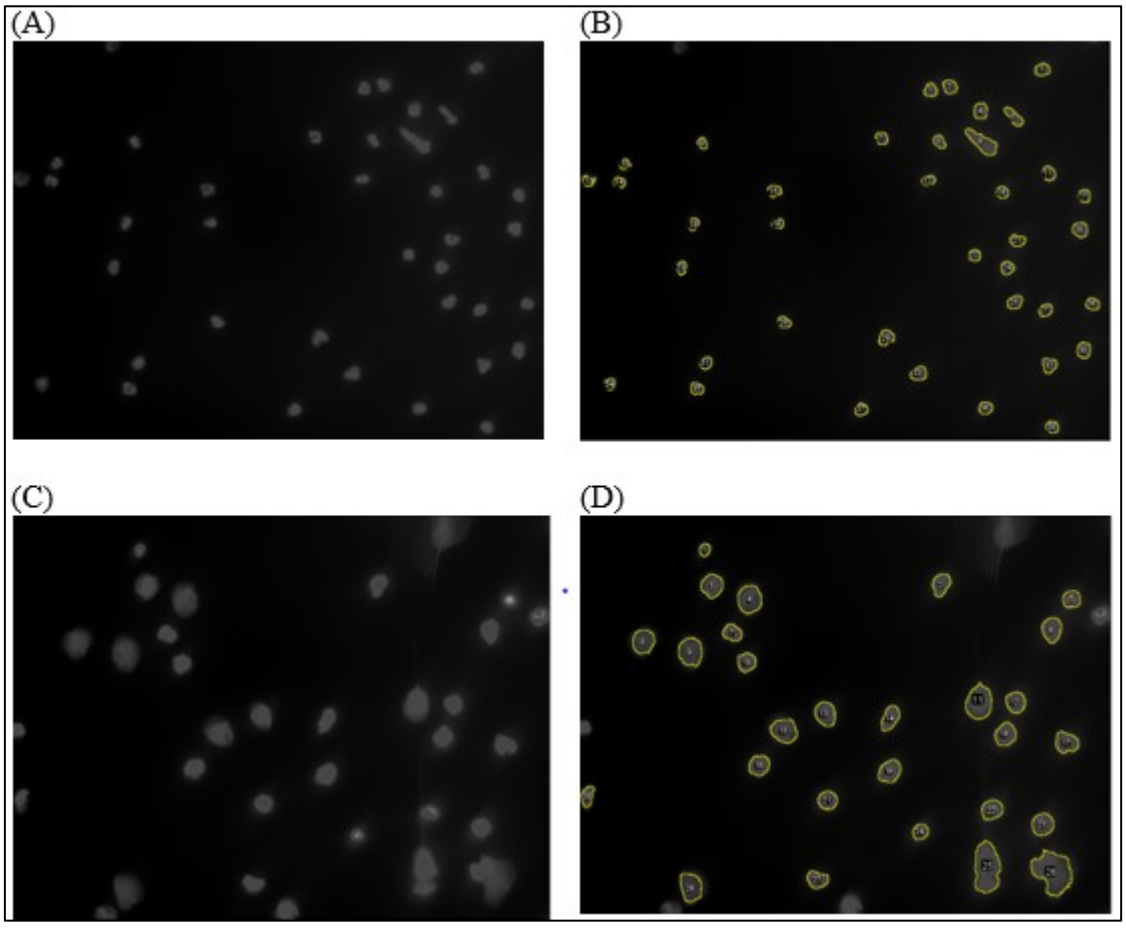

Figure 1. Example images before and after DANA_I. (A-D) Images before and after DANA_I. Analyzing took place in ImageJ/Fiji. (A, B) Untreated cells were left in an incubation medium for two hours at 37°C. (A) Raw image of untreated cells, and (B) after

DANA_I was run. (C, D) Cells were treated with 100 nM PMA. (C) Raw image of PMA-treated cells and (D) after DANA_I was run. DANA_I: DANA: DNA area and NETosis analysis; PMA: phorbol 12-myristate 13-acetate.

First, following the optimization instructions, Fiji plugins for DANA were installed, and for optimal usage in this study, the microscope calibration was adapted to 7,04 in every plugin. In general, there were plugins to analyze images individually on a per cell, per image, and per sample basis, as well as a rapid alternative to analyzing the whole folder per batch plugin. It was easy to create new plugins to analyze all pictures due to different file types, for example, TIF and PNG. For the analysis of our images, the auto-threshold method for ImageJ was changed in these plugins from Li white to intermodes because neutrophil detection worked better for these images. The auto-local threshold was also changed from white to black in every plugin. In addition, the output directory for Microsoft Excel sheets in plugins was adapted to a defined folder on the currently utilized computer.

An optimization Microsoft Excel spreadsheet was available to generate the upper cutoff, lower cutoff, and NETs cutoff for the images used in this study for optimal usage of DANA. Thus, for each image included in the optimization (n = 17), the total number of cells, NETs, and multiples was counted by eye, and the data were entered into the optimization sheet (Figure 2). Images that contained more than seven multiples or did not run accurately were not used in the optimization process (n = 3).

DANA was run on the optimization images to calculate the lower cutoff parameter. DANA advised reviewing these images while considering a lower cutoff if numerous fragments were detected (Figure 2). For these images, 20,000 lower cutoff fit.

After the lower cutoff was defined, DANA was run using the mean area of the five smallest non-outlier ROIs with an upper elimination cutoff of 1.2. From the Microsoft Excel files that DANA_II created, the number of multiples discovered by DANA was placed in the spreadsheet for each image. This procedure was repeated with upper cutoffs of 1.5, 1.8, and 2.1. Next, the absolute difference of multiples identified by eye and DANA was calculated. Then, the average of the absolute differences was determined for each upper cutoff, and the one with the lowest average absolute difference was selected for

quantification. One number between two upper cutoffs was chosen if they produced comparable average absolute differences. In this study, 1.95 was generated.

DANA was again applied to the optimization images using the optimized lower and upper cutoffs. The number of cells with relative areas above 3.00, 4.00, 5.00, 6.00, 7.00, 8.00, 10.00, and 12.00 times was filled in the spreadsheet to generate the NETs cutoff (Figure 2). These values were found in the Microsoft Excel files generated by DANA_II for each image. After the values of 3.00, 4.00, 5.00, and 6.00 were filled in, the same image was run with the adjusted DNA decondensation cutoffs of 7.00, 8.00, 10.00, and 12.00. The total cells for the associated image were then multiplied by the DNA decondensation cutoff parameter closest to the number of NETs visually identified by eye for each image, called the weighted average. The last computation phase divided the total cells by eye of all optimized images by the total weighted average. Subsequently, the closest DNA decondensation cutoff parameter to the number of NETs identified by eye for each image was used to multiply the total cells for the related image. In the last calculation step, the sum of the total NETs of all optimized images was divided by the sum of all optimized cutoffs. In this study, a 4.30 NETs cutoff was applied.

(A)

C	D	E
Total Cells	Total NETs	Multiples
	By eye	
19	16	2
21	19	3
28	24	0
16	11	0
50	34	4
36	26	2
57	46	6
40	36	4
36	1	2
16	1	0
36	0	2
27	0	0
22	0	0
43	1	1
42	0	3
88	2	2
53	1	2

(B)

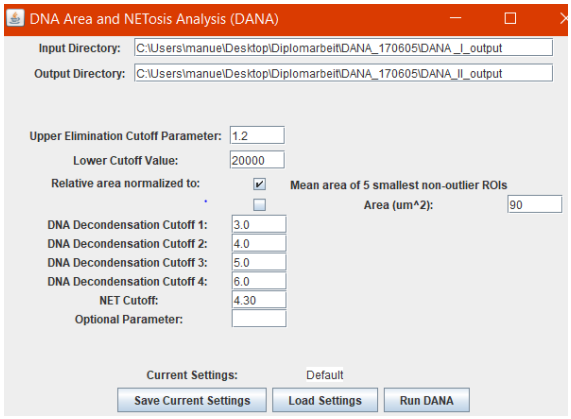

(C)

Multiples		Multiples (Absolute Difference)
	Mean + 1.2SD	
4		2
9		6
6		6
5		5
5		1
3		1
6		0
7		3
0		2
0		0
0		2
0		0
0		0
0		1
0		3
1		1
0		2
	Average;	2,058823529

(D)

3x	4x	5x	6x	7x	8x	10x	12x
			DANA				
18	17	13	10	6	3	1	1
18	18	18	16	13	10	3	2
24	24	22	19	15	12	4	0
11	11	10	9	7	5	3	1
37	29	18	9	4	1	1	0
37	32	19	12	7	4	3	2
57	53	33	21	13	7	1	0
40	38	24	21	10	10	2	1
6	2	2	2	0	0	0	0
3	0	0	0	0	0	0	0
13	1	1	1	1	1	0	0
8	0	0	0	0	0	0	0
5	0	0	0	0	0	0	0
12	2	0	0	0	0	0	0
24	9	3	3	2	1	1	0
20	4	3	2	1	1	1	0
6	3	2	0	0	0	0	0

Figure 2. Optimization workflow (A-D). Screenshots of the optimization workflow taking place in a spreadsheet in Microsoft Excel: (A) Counted total cells, total NETs, and multiples from optimization images (n = 17); (B) DANA software where the upper cutoff, lower cutoff, NETs cutoff, DNA decondensation cutoffs, and the input and output directories could be adjusted to optimize the study's parameters or for data analysis; (C) An illustration of a spreadsheet for creating the upper cutoff similar steps were taken for Mean + 1.5, 1.8, and 2.1 SDs; (D) An illustration for the generation of the NETs cutoff containing the cells for each DNA decondensation cutoff for each image. DANA: DNA area and NETosis analysis; DNA: desoxyribonucleic acid; NETs: neutrophil extracellular traps; SD: standard deviation.

Now, the DANA workflow was applied to calculate the proportion of NETs formation for a single patient (Figure 3). First, a plugin was applied to the raw image in ImageJ/Fiji. Following cell analysis, a Microsoft Excel csv-file with data on the cells in this image was saved in the specified folder on the computer. These steps were repeated for each image of the patient, or a batch plugin could be used, that performed DANA_I on every image in the selected folder. Once more, the data was saved in a unique Microsoft Excel csv-file for each image and placed in the designated output folder. After completing these steps, DANA_II was run on these Microsoft Excel csv-files with the optimized parameters. Therefore, the path to the folder where each patient's Microsoft Excel csv-files were stored was inserted into the input directory, and the output folder needed to be specified. Then, DANA_II calculated the percentage of NETs formation and created a second Microsoft Excel csv-file for every image and a summary file specifically for each patient.

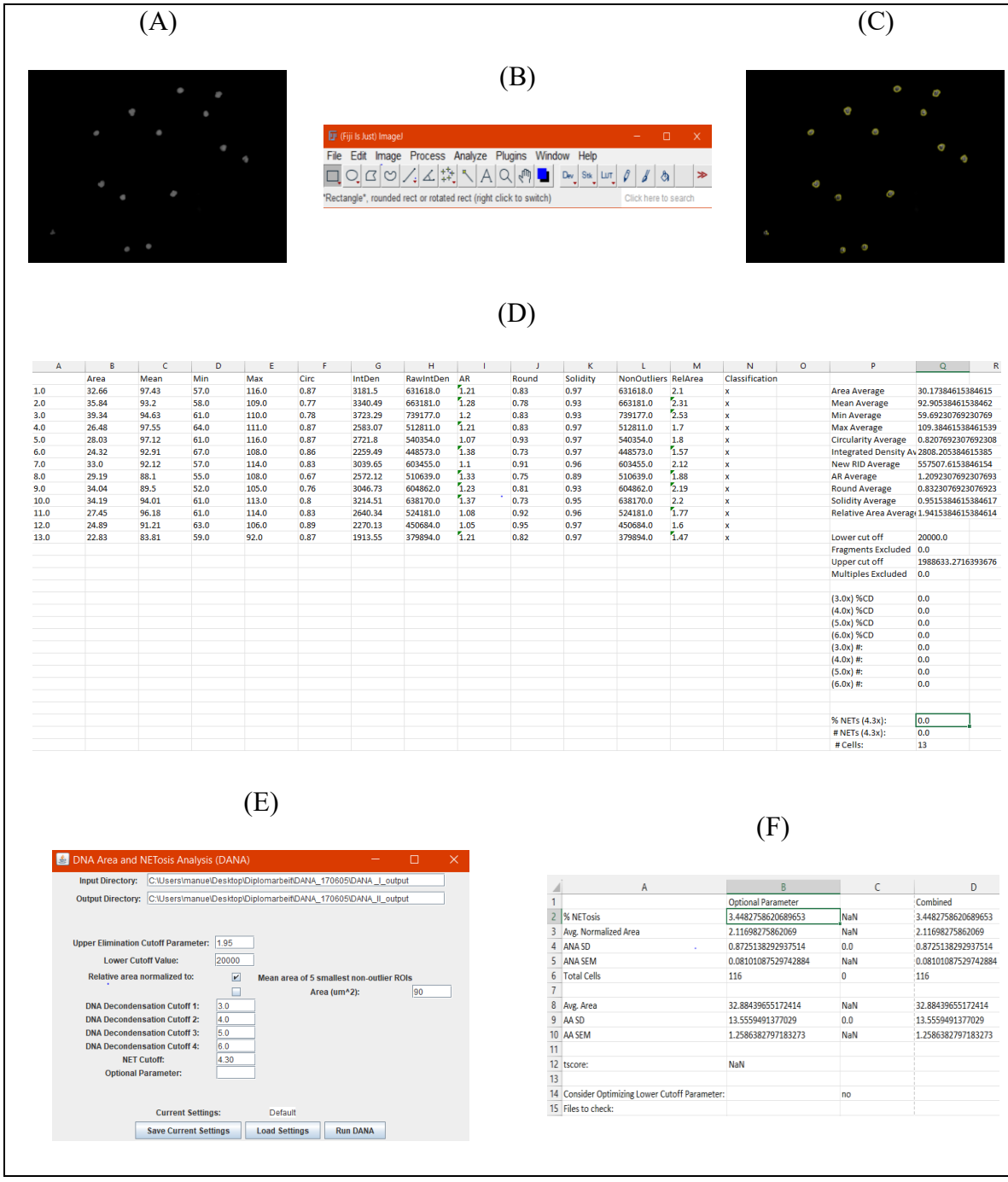

	Area	Mean	Min	Max	Circ	IntDen	RawIntDen	AR	Round	Solidity	NonOutliers	RelArea	Classification		
1.0	32.66	97.43	57.0	116.0	0.87	3181.5	631618.0	1.21	0.83	0.97	631618.0	2.1	x	Area Average	30.17384615384615
2.0	35.84	93.2	58.0	109.0	0.77	3340.49	663181.0	1.28	0.78	0.93	663181.0	2.31	x	Mean Average	92.90538461538462
3.0	39.34	94.63	61.0	110.0	0.78	3723.29	739177.0	1.2	0.83	0.93	739177.0	2.53	x	Min Average	59.69230769230769
4.0	26.48	97.55	64.0	111.0	0.87	2583.07	512811.0	1.21	0.83	0.97	512811.0	1.7	x	Max Average	109.38461538461539
5.0	28.03	97.12	61.0	116.0	0.87	2721.8	540354.0	1.07	0.93	0.97	540354.0	1.8	x	Circularity Average	0.8207692307692308
6.0	24.32	92.91	67.0	108.0	0.86	2259.49	448573.0	1.38	0.73	0.97	448573.0	1.57	x	Integrated Density Av	2808.20538615385
7.0	33.0	92.12	57.0	114.0	0.83	3039.65	603455.0	1.1	0.91	0.96	603455.0	2.12	x	New RID Average	557507.6153846154
8.0	29.19	88.1	55.0	108.0	0.67	2572.12	510639.0	1.33	0.75	0.89	510639.0	1.88	x	AR Average	1.2092307692307693
9.0	34.04	89.5	52.0	105.0	0.76	3046.73	604862.0	1.23	0.81	0.93	604862.0	2.19	x	Round Average	0.8323076923076923
10.0	34.19	94.01	61.0	113.0	0.8	3214.51	638170.0	1.37	0.73	0.95	638170.0	2.2	x	Solidity Average	0.9515384615384617
11.0	27.45	96.18	61.0	114.0	0.83	2640.34	524181.0	1.08	0.92	0.96	524181.0	1.77	x	Relative Area Average	1.9415384615384614
12.0	24.89	91.21	63.0	106.0	0.89	2270.13	450684.0	1.05	0.95	0.97	450684.0	1.6	x		
13.0	22.83	83.81	59.0	92.0	0.87	1913.55	379894.0	1.21	0.82	0.97	379894.0	1.47	x	Lower cut off	20000.0
														Fragments Excluded	0.0
														Upper cut off	1988633.2716393676
														Multiples Excluded	0.0
														(3.0x) %CD	0.0
														(4.0x) %CD	0.0
														(5.0x) %CD	0.0
														(6.0x) %CD	0.0
														(3.0x) #:	0.0
														(4.0x) #:	0.0
														(5.0x) #:	0.0
														(6.0x) #:	0.0
														% NETs (4.3x):	0.0
														# NETs (4.3x):	0.0
														# Cells:	13

	A	B	C	D
1		Optional Parameter		Combined
2	% NETosis	3.4482758620689653	NaN	3.4482758620689653
3	Avg. Normalized Area	2.11698275862069	NaN	2.11698275862069
4	ANA SD	0.8725138292937514	0.0	0.8725138292937514
5	ANA SEM	0.08101087529742884	NaN	0.08101087529742884
6	Total Cells	116	0	116
7				
8	Avg. Area	32.88439655172414	NaN	32.88439655172414
9	AA SD	13.5559491377029	0.0	13.5559491377029
10	AA SEM	1.2586382797183273	NaN	1.2586382797183273
11				
12	tscore:	NaN		
13				
14	Consider Optimizing Lower Cutoff Parameter:		no	
15	Files to check:			

Figure 3. DANA workflow algorithm from raw image to the percentage of NETs formation per patient. (A-F) Steps for calculating the percentage of NETs formation for a patient with DANA. (A-D) Algorithm steps for DANA_I: (A) Example image of untreated cells. Cells were left in an incubation medium for 2 hours at 37°C; (B) ImageJ/Fiji software (C) analyzed cells after threshold; (D) A related Microsoft Excel csv-file containing all the information for the cells in this image (A-D) could be run on each image individually for one patient or could be simplified using batch plugin, and DANA_I was run on each image in the selected folder. (E, F) Algorithm steps for DANA_II: (E)

DANA_II software; (F) Summary sheet of the patient, including information from all generated Microsoft Excel csv-files from DANA_II. DANA: DNA area and NETosis analysis.

Images from ten patients were selected to validate the method and see how comparable analysis by DANA with analysis by eye was. The percentage of NETs formation was calculated by eye for every patient for every condition (i.e., incubation medium, *E. coli*, PMA). The percentage of NETs formation was calculated by dividing the number of NETs-like structures by the total number of cells (intact neutrophils + NETs-like structures) multiplied by 100. Then, DANA was run on these patients´ images, and the data was compared (Figure 4). The NETs formation counted by DANA and counted by eye was not significantly different for each condition (Table 1).

Table 1. Validation of DANA vs. Counting by eye (n = 10).

		Mean (%)	Standard deviation (%)	p-value paired t-test
Control	DANA	11.82	19.31	p = 0.264
	by eye	4.763	6.473	
E. coli	DANA	24.18	10.31	p = 0.457
	by eye	26.59	8.048	
PMA	DANA	61.62	12.39	p = 0.085
	by eye	70.21	22.58	

DANA: DNA area and NETosis analysis; PMA: phorbol 12-myristate 13-acetate.

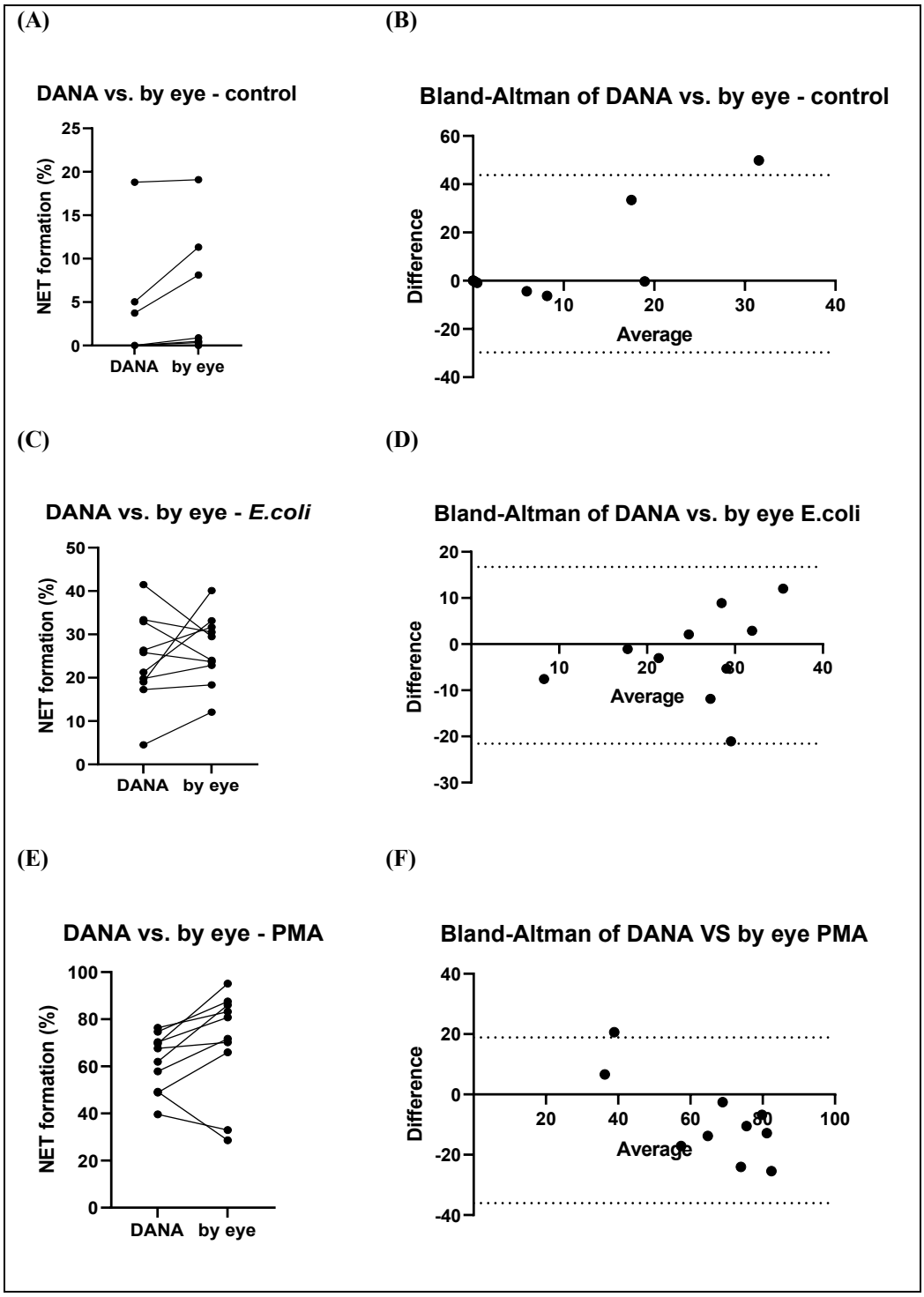

Figure 4. Comparison of NETs formation percentage by DANA and by eye to validate DANA. Neutrophils were (A, B) as a control condition left in an incubation medium for 2 hours at 37°C and treated with (C, D) heat-inactivated *E. coli* (250 bacteria/cell) or with (E, F) 100 nM PMA. A Bland Altman and paired t-test were performed to compare the percentage of NETs formation by eye and DANA. (A) Comparison in the control condition ($p = 0.264$); (B) Bland-Altman in the control condition; (C) Comparison in the *E. coli*

condition (p = 0.457); (D) Bland-Altman in *E. coli* condition; (E) Comparison in the PMA condition (p = 0.085); (F) Bland-Altman in the PMA condition. DANA: DNA area and NETosis analysis; PMA: phorbol 12-myristate 13-acetate.

3.2 Calculation time

As expected, there was a significant difference (p = 0.006) in comparing the calculation time of NETs formation among patients (n = 7) calculated by eye and with DANA (Figure 5; Figure 6). The longest calculation time by eye was 50 minutes, whereas with DANA, the longest was about 6 minutes. On average, counting by eye took 30 minutes, which decreased to 5 minutes when DANA was used (Table 2).

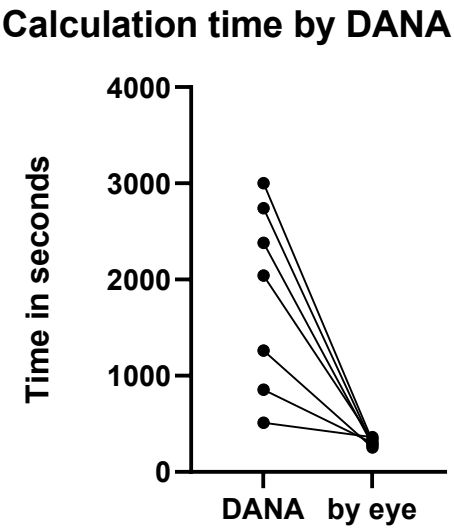

Figure 5. Comparison of calculation time by DANA and by eye. There was a significant difference in calculation time by DANA and by eye among patients (n = 7). For the comparison, a paired t-test was applied (p = 0.006). DANA: DNA area and NETosis analysis.

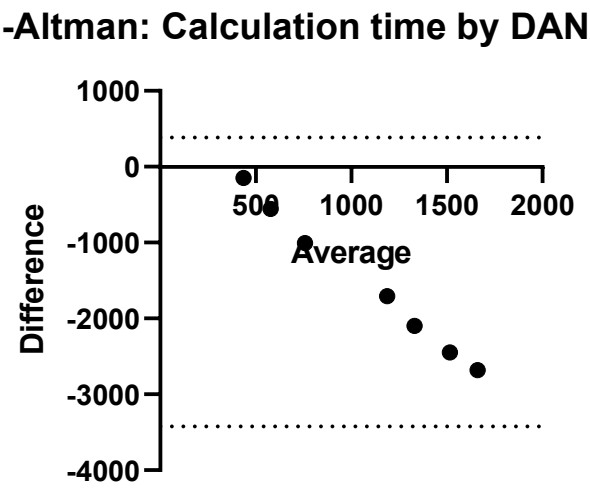

Figure 6. Bland-Altman comparing calculation time by DANA vs. by eye.

Table 2. Time calculation of NETs formation by DANA and by eye (n = 7) in seconds.

	By eye	DANA
Minimum	510	255
Maximum	3000	363
Range	2490	108
Mean	1826	306.3
Standard deviation	962.8	35.82

DANA: DNA area and NETosis analysis.

3.3 Patients' characteristics

To further control our data before comparing NETs formation, the patients' selection algorithm (Figure 7) was used for quality control. This algorithm was applied to each patient in each condition. There, it was determined whether duplicates were available for analysis, whether there was a coefficient of variation above 30% between the duplicates in the percentage of NETs formation, and whether DANA correctly detected cells.

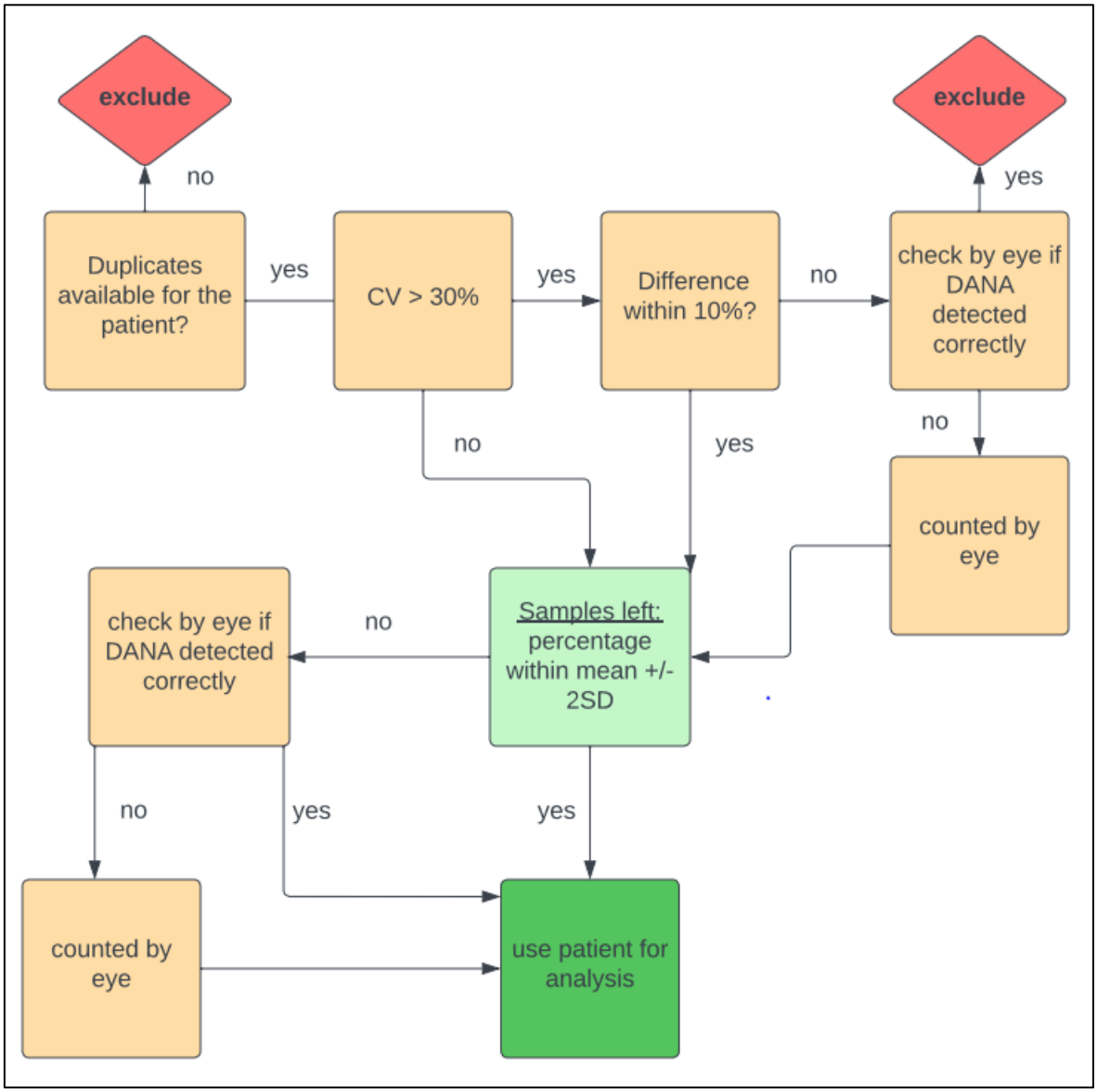

Figure 7. Patients' selection algorithm made with Lucidchart can be found on the Lucidchart website: [Von der Visualisierung zur Umsetzung | Lucidchart]. Here, the algorithm was presented to determine which data was excluded from the analysis. First, it was checked if two different slides were available to analyze. Then, the CV of the

percentage of NETs formation in these two different slides was calculated. The absolute difference between the duplicates was checked to see if it was within 10% if the CV was higher than 30%. If not, it was examined to see if DANA accurately spotted the cells. If DANA accurately identified them, they were taken out of the analysis. If they could not be detected well enough, they were manually counted, and the results were used for the next steps. The mean +/- 2 standard deviation was then computed independently for each condition and group. The duplicates were examined to determine whether DANA correctly identified the cells when the percentage of NETs formation patients did not fall within the mean +/- 2 standard deviation. If so, the data were used for analysis; if not, the patient's condition was counted visually by eye and considered. CV: coefficient of variation; DANA: DNA area and NETosis analysis.

Pictures of 121 patients were available. Before the patient's selection algorithm for quality control was applied (Figure 7), 10 patients were ruled out because it was unclear whether they suffered from sarcopenia, LC, or both. The patients were then subjected to the patient's selection algorithm (Figure 7) for each condition (i.e., control condition, *E. coli*, PMA). There were nine patients excluded because there were no duplicates in any condition. Furthermore, 2 patients were excluded because the coefficient of variation was above 30% in every condition. After the patients' selection algorithm, pictures of 100 different patients were available.

Patients were divided into the groups of liver cirrhosis + sarcopenia (LC + S) (n = 58), LC without sarcopenia (n = 26) and sarcopenia without LC (n = 16). The mean age of patients in group LC + S was 61.93 +/- 12.15 years, in group LC 60.69 +/- 12.67 years, and in group sarcopenia 60.56 +/- 14.46 years (Table 3). There was no difference in age (Figure 8) between the groups analyzed with the Kruskal-Wallis test ($p = 0.905$).

Table 3. Patients' characteristics of the groups LC + S, LC, and S.

	LC + S	LC	S
Number of values (n)	58	26	16
Minimum of age	28.00	19.00	26.00
Maximum of age	85.00	77.00	79.00
Range of age	57.00	58.00	53.00
Mean of age	61.93	60.69	60.56
Standard deviation of age	12.15	12.67	14.46
Number of males	47	13	9
Number of females	11	13	7

LC + S: liver cirrhosis + sarcopenia; LC: liver cirrhosis; S: sarcopenia.

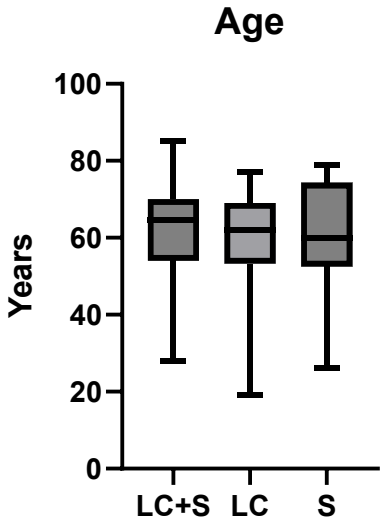

Figure 8. Comparison of age in years between the groups. There was no significant difference in age between groups using the Kruskal-Wallis test (p = 0.905). LC + S: liver cirrhosis + sarcopenia; LC: liver cirrhosis; S: sarcopenia.

A bigger proportion of male patients was in the LC + S group when comparing the three groups according to their sex distribution (Figure 9). Divided into groups: 58 patients in group LC + S, 47 (81%) were male and 11 (19%) were female; 13 patients in the group LC (50%) were male and 13 (50%) were female; 16 patients in the group S, 9 (56%) were male and 7 (43%) were female.

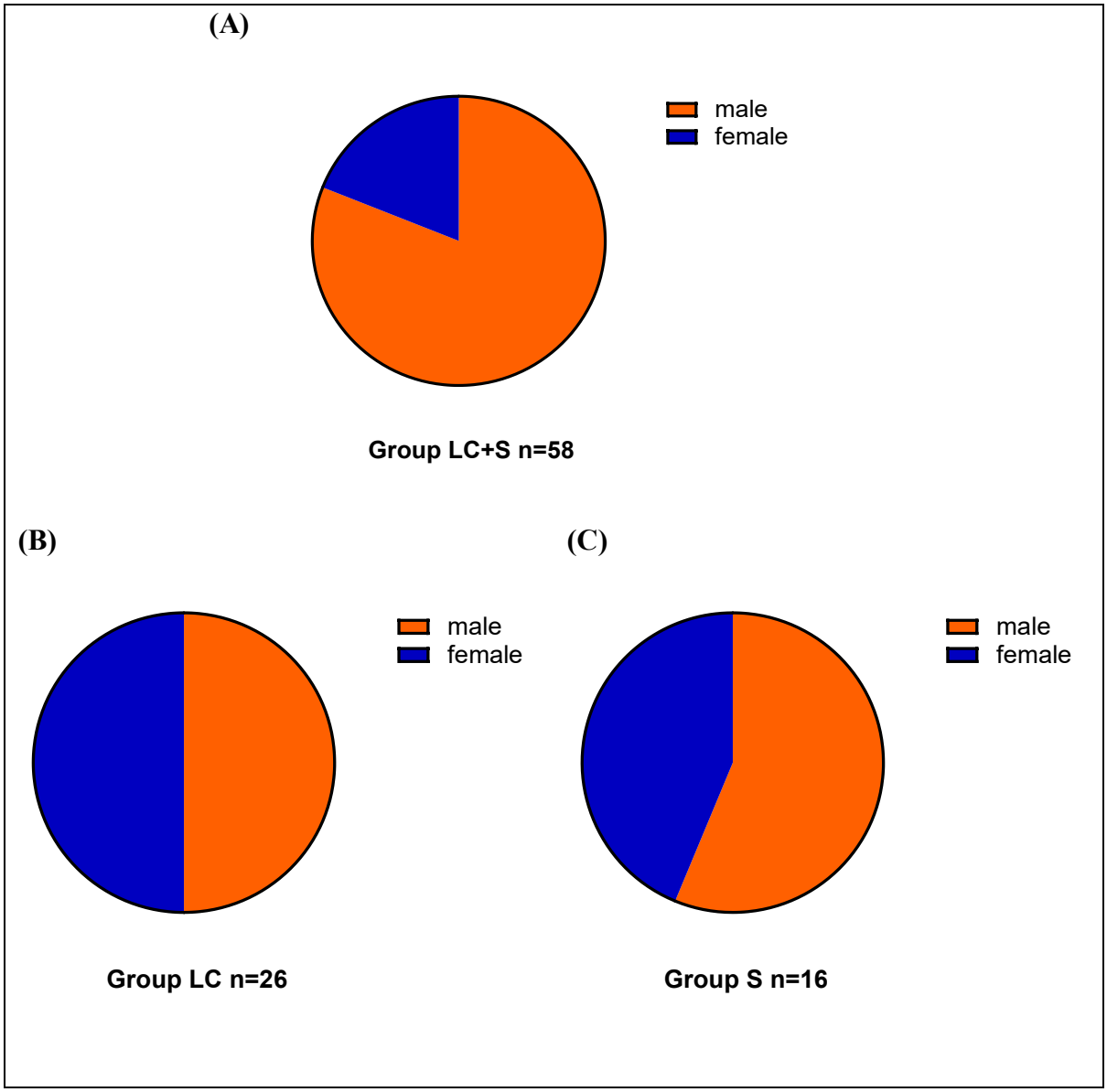

Figure 9. Sex of patients in different patients' groups. There was a significant difference in sex distribution using *the c*hi-square test (p = 0.0085). (A) Sex distribution of

group LC + S; (B) Sex distribution of LC; (C) Sex distribution of group S. LC + S: *l*iver cirrhosis + sarcopenia; LC: *l*iver cirrhosis; S: *s*arcopenia.

3.3 NETs formation analysis in patients' samples

3.3.1 Spontaneous NETs formation (unstimulated neutrophils)

After using the patients' selection algorithm (Figure 7), data from 41 patients were available in group LC + S, 21 in group LC, and nine in group with sarcopenia only. Figure 10 shows example images of neutrophils without stimulation in each group.

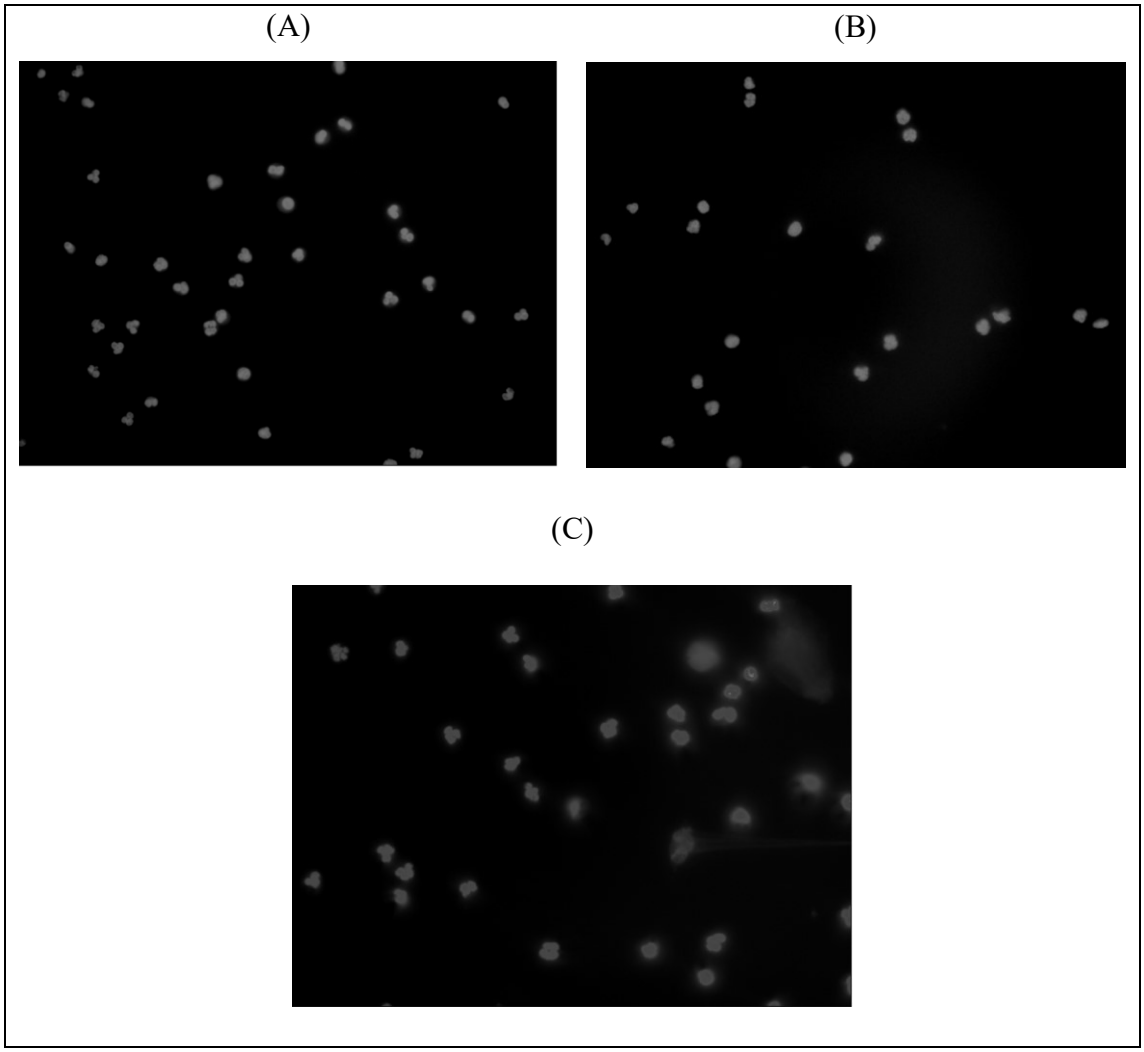

Figure 10. Examples of pictures analyzed of spontaneous NETs formation. (A-C) Raw images of neutrophil granulocytes, which were left in an incubation medium for 2 hours at 37°C: (A) Image of unstimulated neutrophils of a patient in group LC + S; (B) group LC;

and (C) of a patient with sarcopenia. LC + S: liver cirrhosis + sarcopenia; LC: liver cirrhosis; NETs: neutrophil extracellular traps.

The average percentage of NETs formation in the group LC + S was 14.45 +/- 18.68; in the group LC without sarcopenia, 18.80 +/- 21.27; and in the group sarcopenia without LC, 37.50 +/- 28.17 (Table 4).

Table 4. Spontaneous NETs formation.

NETs formation (%): Control condition			
	LC + S	**LC**	**S**
Number of samples (n)	41	21	9
Minimum	0.000	0.000	1.725
Maximum	68.55	66.39	77.14
Range	68.55	66.39	75.41
Mean	14.45	18.80	37.50
Standard deviation	18.68	21.27	28.17

LC + S: liver cirrhosis + sarcopenia; LC: liver cirrhosis; S: sarcopenia; NETs: neutrophil extracellular traps.

No statistically significant difference was found in the Kruskal-Wallis test analysis in the control condition ($p = 0.056$). Although the NETs formation was not significantly different between the groups, there was a tendency toward increased NETs formation observed in group S compared to LC + S ($p = 0.049$) and LC ($p = 0.232$) after Dunn's post hoc analysis (Figure 11).

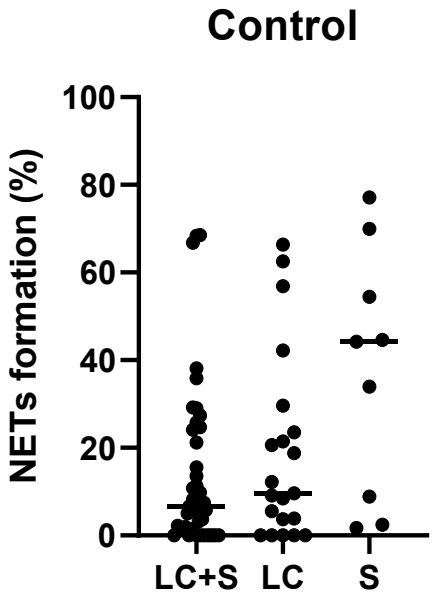

Figure 11. Comparison of NETs formation between the groups in the control condition. Neutrophils were left in an incubation medium for two hours at 37°C. There was a tendency of increased spontaneous NETs formation in group S; however, there was no statistical significance if the Kruskal-Wallis test was performed ($p = 0.056$; after Dunn's post hoc analysis sarcopenia compared to LC + S ($p = 0.049$) and LC ($p = 0.232$)). LC + S: liver cirrhosis + sarcopenia; LC: liver cirrhosis; S: sarcopenia; NETs: neutrophil extracellular traps.

3.3.2 NETs formation upon stimulation with *E. coli*

After using the patients' selection algorithm (Figure 7), data from 37 patients in group LC + S, 19 patients in group LC, and ten patients with sarcopenia were available. Figure 12 shows examples of NETs formation upon stimulation with *E. coli* in this study.

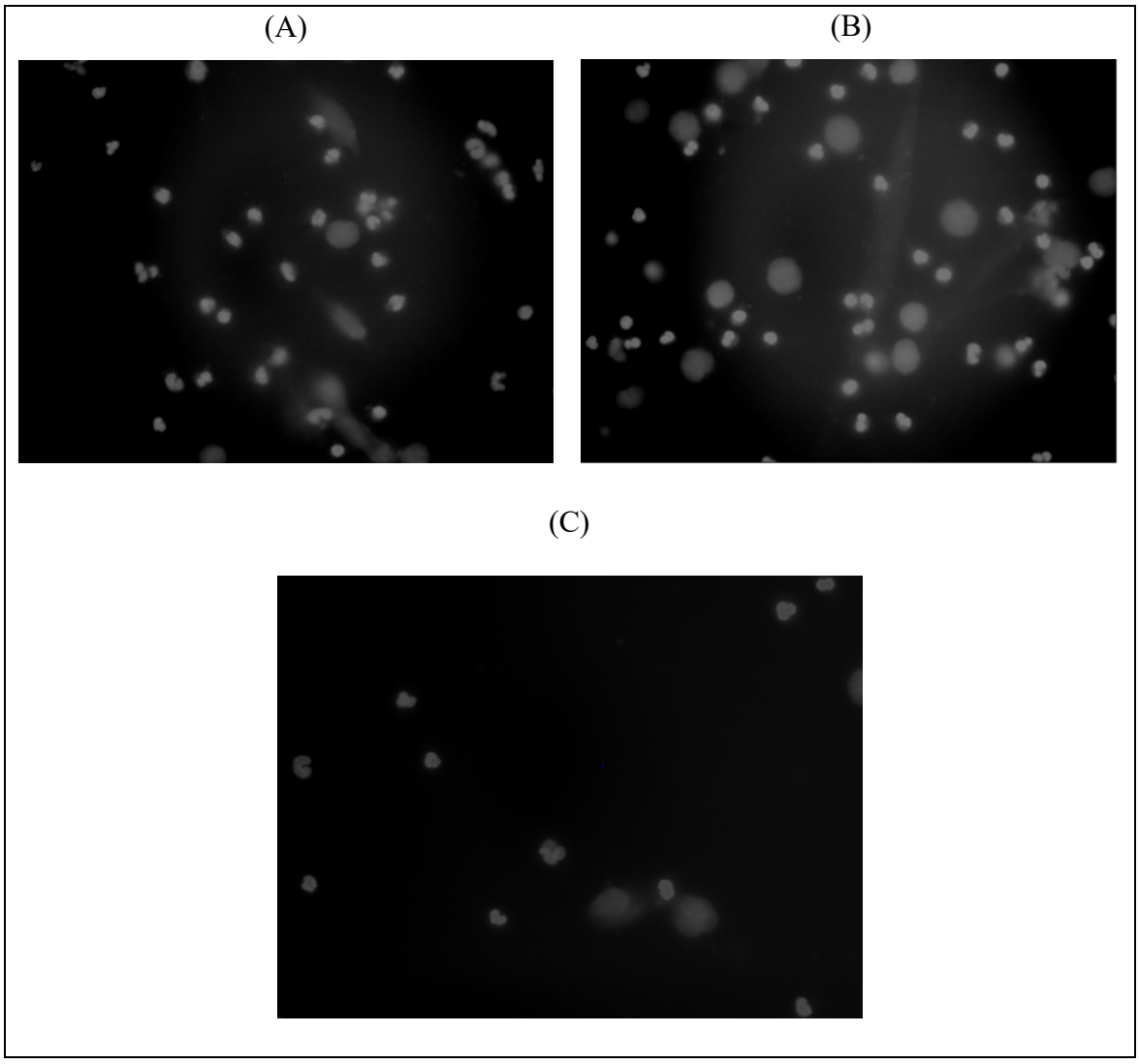

Figure 12. Examples of pictures analyzed of NETs formation upon stimulation with *E. coli*. (A-C) Raw images of neutrophil granulocytes stimulated with heat-inactivated *E. coli* (250 bacteria/cell). (A) Images of neutrophils upon stimulation with *E. coli* of a patient in group LC + S, (B) group LC, and (C) sarcopenia. LC + S: liver cirrhosis + sarcopenia; LC: liver cirrhosis; NETs: neutrophil extracellular traps.

The mean percentage of neutrophils undergoing NETosis was 35.56 +/- 28.44 for patients with both LC and sarcopenia, 35.29 +/- 26.44 for patients with LC without sarcopenia, and 29.70 +/- 26.09 for patients with sarcopenia without LC (Table 5).

Table 5. NETs formation upon stimulation with E. coli.

NETs formation (%): *E. coli* condition			
	LC + S	**LC**	**S**
Number of samples (n)	37	19	10
Minimum	0.000	4.435	0.000
Maximum	92.77	86.07	68.78
Range	92.77	81.64	68.78
Mean	35.56	35.29	29.70
Standard deviation	28.44	26.44	26.09

LC + S: liver cirrhosis + sarcopenia; LC: liver cirrhosis; S: sarcopenia.

Figure 13 shows a comparison between the groups in terms of the percentage of NETs formation upon stimulation with *E. coli*. There was no significant difference observed using the Kruskal-Wallis test between the groups in NETs formation ($p = 0.778$).

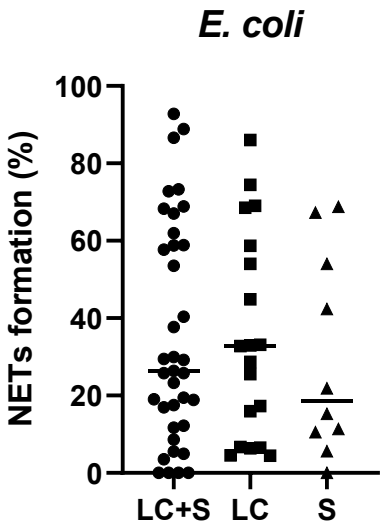

Figure 13. NETs formation upon stimulation with *E. coli* between the groups of patients. Neutrophil granulocytes were stimulated with heat-inactivated *E. coli* (250 bacteria/cell). No statistical significance was found if Kruskal-Wallis test was performed ($p = 0.778$). LC + S: liver cirrhosis + sarcopenia; LC: liver cirrhosis; S: sarcopenia; NETs: neutrophil extracellular traps.

3.3.3 NETs formation upon stimulation with PMA

After exclusion using the patients' selection algorithm (Figure 7), 37 patients had data in group LC + S, 22 in group LC, and 11 in group sarcopenia (Table 6). Figure 14 shows examples of pictures analyzed in this study upon stimulation of neutrophil granulocytes with PMA.

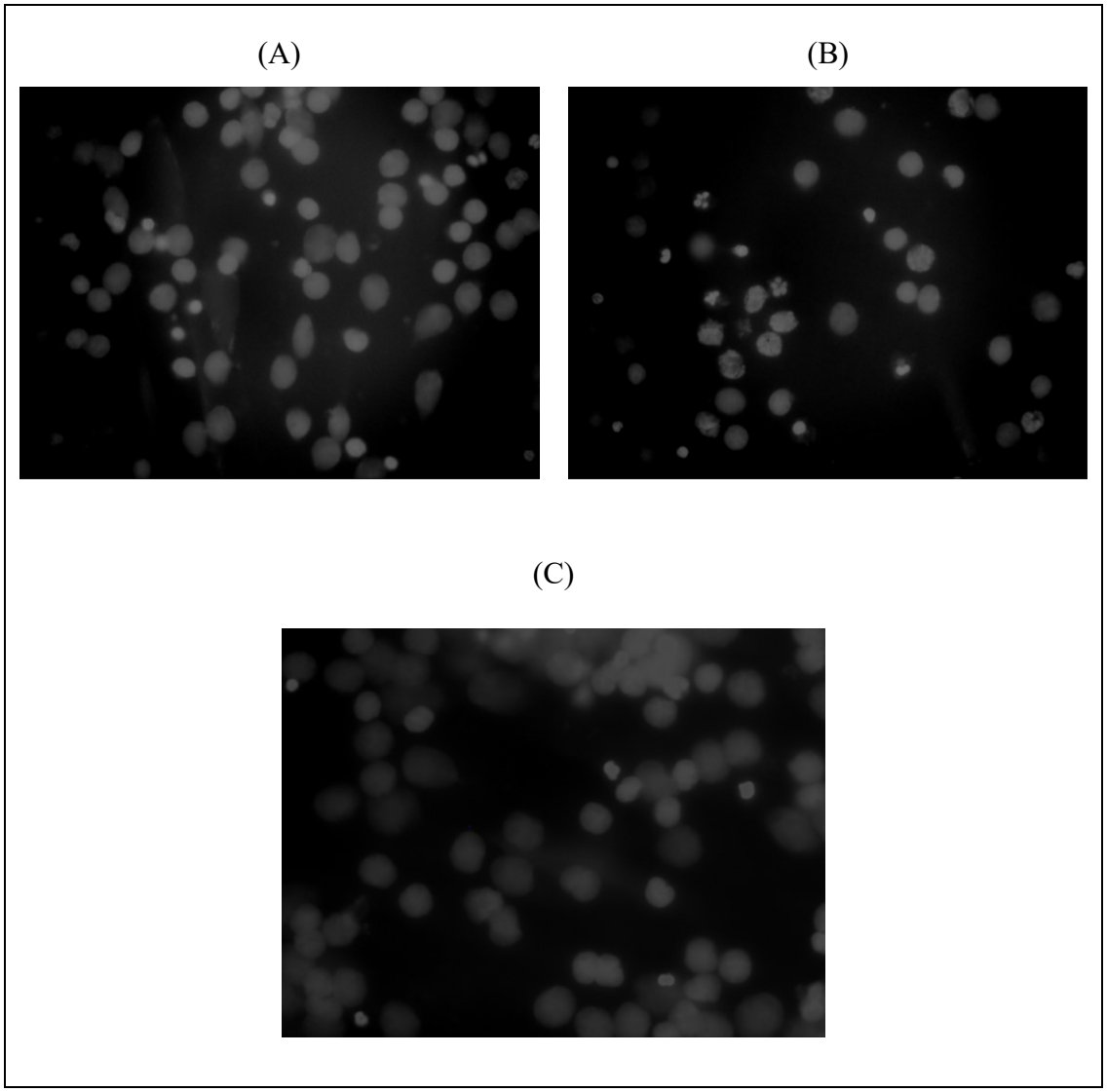

Figure 14. Examples of pictures analyzed of NETs formation upon stimulation with PMA. Neutrophil granulocytes were stimulated with PMA (100 nM). (A) shows one picture of a patient with LC + S; (B) shows one picture of a patient in group LC; (C) shows one picture of a patient with sarcopenia. LC + S: liver cirrhosis + sarcopenia; LC: liver cirrhosis; NETs: neutrophil extracellular traps; PMA: phorbol 12-myristate 13-acetate.

The mean percentage for patients with LC and sarcopenia was 47.75 +/- 29.10, for patients with LC without sarcopenia 56.20 +/- 24.89, and for patients with sarcopenia without LC it was 50.53 +/- 26.81 (Table 6).

Table 6. NETs formation upon PMA stimulation.

NETs formation: PMA condition			
	LC + S	**LC**	**S**
Number of samples (n)	37	22	11
Minimum	0.000	6.250	0.000
Maximum	93.58	92.87	75.55
Range	93.58	86.62	75.55
Mean	47.75	56.20	50.53
Standard deviation	29.10	24.89	26.81

LC + S: liver cirrhosis + sarcopenia; LC: liver cirrhosis; S: sarcopenia. NETs: neutrophil extracellular traps; PMA: phorbol 12-myristate 13-acetate.

Figure 15 shows a comparison of the percentage of NETs formation upon stimulation with PMA between groups. There was no statistically significant difference found using the Kruskal-Wallis test ($p = 0.490$).

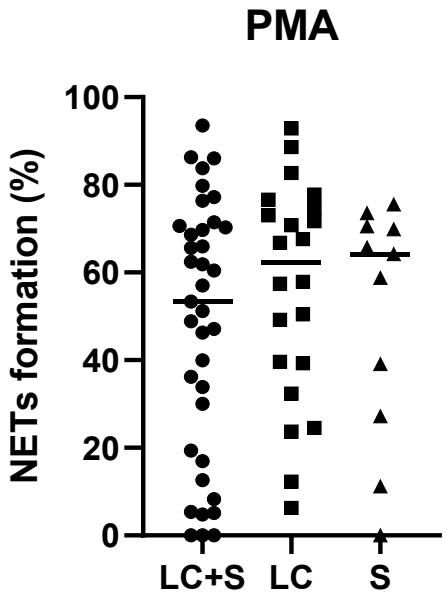

Figure 15. NETs formation upon stimulation with PMA. Neutrophil granulocytes were stimulated with PMA (100 nM). No statistical significance was found if Kruskal-Wallis test was performed (p = 0.490). LC + S: liver cirrhosis + sarcopenia; LC: liver cirrhosis; S: sarcopenia; NETs: neutrophil extracellular traps; PMA: phorbol 12-myristate 13-acetate.

4 Discussion

Recently discovered NETs formation to capture and eliminate pathogens has become an active field of research in neutrophil biology in the last few years. Notably, the ability of NETs to damage host tissue through the release of cytotoxic substances and the significance of NETs developing therapeutic strategies for chronic inflammation have attracted recent attention. Since LC still has high morbidity and mortality, and sarcopenia is associated with an approximately two times higher risk of death in patients with LC (16), the need for novel therapeutic interventions exists. LC and sarcopenia are diseases highly associated with chronic inflammation and alterations in the immune system (18, 1, 7). However, the role of NETs in their pathogenesis and as a potential therapeutic target has not been well described.

Within this study, we aimed to investigate the NETs formation function in patients with sarcopenia and LC. To our knowledge, no study has examined NETs in sarcopenia, and little is known about their role in patients with LC either. Furthermore, since quantifying and analyzing the percentage of NETs in microscope images by eye can be a laborious and time-consuming assignment, we alternatively aimed to implement artificial intelligence (AI).

Therefore, DANA was chosen as a semiautomated published method for analyzing microscope images utilizing a single fluorescent channel. DANA is cost-effective, easy to implement even without programming skills, and applicable for different cells and image types on a per cell, per image, per sample basis with direct visualization. Due to its robustness, the results can be replicated across laboratories. It allows rapid quantification of the percentage of NETs formation per patient and, compared to counting by eye, can reduce unintentional bias, inconsistency over time, and subjectivity (41). After successful optimization and validation of DANA, it was possible to decrease the mean time of analysis from 30 to 5 minutes per patient if the percentage of NETs formation was counted by eye compared to DANA ($p = 0.006$). Notably, the calculation time by eye highly depends on the number of cells in the images.

The disadvantages of DANA are that optimization could still require a considerable amount of human effort, and confirmation with NETs markers may be required (42). This study used DAPI to dye neutrophils without further immunostaining using antibodies

against MPO, NE, or H3Cit. However, cationic molecules can hamper the binding of DNA-intercalating dyes with NETs and limit their visualization. Furthermore, DNA-intercalating dyes may not differ between necrotic cells and NETs. Thus, some researcher have recommended additional antibody techniques (43).

Nonetheless, a further immunostaining step involving the co-localization of proteins specific to neutrophils is not always beneficial and may restrict quantification. It can also complicate quantification while limiting flexibility. For instance, NETs and resting neutrophils both contain MPO (41). Results based on cfDNA and MPO-DNA measurements also must be interpreted with caution because cfDNA can be elevated in apoptosis, tissue injury, and necrosis without NETs formation (44). MPO-DNA can also be elevated without NETs formation (33). H3Cit has been considered the most specific thus far (44), but PAD4-independent pathways have not been detected (45). To examine DAPI-stained neutrophils and their co-localization with MPO or elastase, NETQUANT, an automated immunostaining quantification approach, was published. For instance, the NETs area, nucleus deformation, a rise in the DNA:NETs bound protein ratio, and the DNA/NETs area are all measured there. It is robust, simple to use, adaptable, and rapid (46). A huge benefit is that single NETs can be distinguished when contacting each other. The disadvantage is that the software requires a license (42) and can be altered by anyone (43).

Regarding alternative methods for NETs quantification, flow cytometry and microscopy imaging flow cytometry can provide robust, quick, and sensitive NETs detection but cannot completely replace immunofluorescence microscopy since they cannot detect neutrophils that have already undergone NETosis. They are also more technical and challenging to implement. An advantage is that they can differentiate between vital and suicidal NETosis (42).

One semi-automated method (47) and one fully automated supervised machine learning algorithm to detect NETs (48) exist (42). Important to mention is that the fully automated method only uses PMA-stimulated NETs so far and is highly technical. Transmission and scanning electron microscopy are advantageous to distinguish between necrosis and NETs, but automated methods for quantification are not yet accessible (42). However, unreliable methodologies have hampered the interpretation of often contradictory results (48). To

assess how NETs work in health and contribute to disease, advanced and standardized automated methods to quantify and assays to visualize NETs are necessary.

To examine the role of NETs formation in LC and sarcopenia, neutrophils from 100 patients were observed, which, to our knowledge, had never been studied in such a big clinical study using a semiautomated technique with direct visualization.

Considering the results in detail, while the analysis did not reach statistical significance (Kruskal-Wallis test: $p = 0.056$), there was a tendency toward increased spontaneous NETs formation in the control condition, where neutrophils were left in an incubation medium for 2 hours at 37°C. Sytox-stained neutrophils from the peripheral blood of healthy individuals showed up to 10% spontaneous NETs formation (41). Comparatively, we discovered similar values for LC + S and the LC group, but sarcopenia tended toward higher spontaneous NETs formation.

One theory for higher spontaneous NETs formation in the sarcopenia group is an enhanced low-grade chronic systemic pro-inflammatory state with aging, known as inflammaging, brought on by the impairment of the aging immune system (7). Neutrophil function is known to develop impaired phagocytosis, superoxide production, and NETs generation in older people (49). In older age, neutrophils have been shown to migrate with reduced chemotaxis and less accuracy, hypothesizing that this supports low-grade chronic inflammation and potential collateral damage, further leading to the loss of muscle fibers and reduced muscle quality. PI3K inhibition as a targeted signaling pathway was shown to correct this defect and restore migratory accuracy (8, 19).

Speculating that both groups with LC showed fewer spontaneous NETs than the sarcopenia group alone, some downregulating mechanism may affect NETs formation. In patients with LC, CAID depicts significant immune system abnormalities that result in systemic inflammation, including neutrophil dysfunction and impaired capability to form NETs (18). In the literature, a decrease in the capability of NETs formation *in vitro* was observed according to complications of LC compared to a healthy group (36). It later also showed a decrease in NETs formation in fluid ascites and peripheral blood *in vitro* in patients with LC and SBP compared to healthy ones (37). Notably, these findings were based on PMA stimulation, as we did not find any significant difference in our study in

PMA-stimulated neutrophils (p = 0.490). However, this outcome could be because, in our study, the degree of LC according to severity was not further differentiated.

Contrarily, patients with LC (Child-Pugh B and C) were discovered to have increased NETs markers MPO-DNA and H3Cit-DNA. In contrast, similar NETs markers were found in LC (Child-Pugh A) and healthy individuals, indicating that the severity of the disease may lead to higher systemic inflammation and increased neutrophil dysfunction, including NETs formation. One explanation for the discrepancy could be that although NETs formation is decreased in decompensated LC, NETs markers may remain in circulation due to sustained chronic systemic inflammation (33). The levels of cfDNA and MPO-DNA were higher in patients with LC in acute decompensation and ACLF compared to healthy controls. However, differences between acute decompensation and ACLF were not further observed (38).

One study focusing on NETs in non-alcoholic steatohepatitis found elevated MPO-DNA in the serum of patients with NASH compared to patients with normal liver histology (40). Another study showed elevated circulating NE, H3Cit, and MPO levels in patients with LC suffering from portal vein thrombosis compared to patients with LC without PVT (50). These findings suggest that, on the one hand, there is an association of NETs with thrombotic events and, on the other hand, increased NETs formation in LC if complications are present.

To combine deliberations, although NETs formation in sarcopenia is unexplored, it could be hypothesized that higher spontaneous NETs formation may contribute to sarcopenia. There is growing evidence that inflammation may play a role in the development of sarcopenia (7), emphasizing the importance of further studies on how potentially altered NETs formation may harm muscle tissue. However, a possible overestimation of DANA in this group cannot be ruled out.

Furthermore, there was no significant difference between the groups comparing NETs formation upon stimulation with heat-inactivated *E. coli* (250 bacteria/cell; Kruskal-Wallis test: p = 0.778) and PMA (100 nM; Kruskal-Wallis test: p = 0.490). It could be possible that only the spontaneous generation of NETs formation is increased in sarcopenia, not the capability to form NETs by stimuli. This higher percentage of spontaneous NETs formation may further harm the muscle due to their potentially toxic substances in patients

with sarcopenia. One study quantified NETs formation capability upon PMA stimulation using fluorometry in up to 65% of 20 healthy donors and up to 40% of 20 patients suffering from LC without further complications like ascites fluid and SBP (36).

Since the first description of NETs formation in 2004 (23), NETs and their toxic potential have been linked to various illnesses. NETs seem to promote venous thrombosis (51, 52). NETs degradation can be delayed in the absence of particular host DNases, further demonstrating intravascular clots containing NETs leading to vascular occlusion in patients with sterile neutrophilia and septicemia (53). NETs are also a field of research in systemic autoimmune and autoinflammatory diseases like rheumatoid arthritis (54, 55), systemic lupus erythematosus (54), antineutrophil cytoplasmic antibody (ANCA)-associated vasculitis, antiphospholipid antibody syndrome, and idiopathic inflammatory myopathies (54). NETs degradation capability is associated with lupus nephritis and severe systemic lupus erythematosus (56). Plaque development in atherosclerosis appears to be significantly influenced by NETs (57, 58). The involvement of NETs in inflammatory bowel diseases was studied (59), and evidence is growing that NETs formation influences cancer development (30).

Potential therapeutic approaches are already in use to reduce or degrade NETs formation. DNase targeting DNA, for example, is in clinical use for cystic fibrosis and SLE, as well as N-acetylcysteine, which can reduce NETs formation in liver injury (30). Blocking NETs formation by targeting DNase or inhibiting PAD4 can reduce HCC growth in mice (40). DNase 1 treatment in mice further showed prevention against deep vein thrombosis (60, 61). Moreover, blocking PAD4 prevents deep vein thrombosis. One crucial point is the possibility of adverse effects on the immune system if NETs formation is inhibited (62).

One limitation of this study could be that we did not examine changes in NETs formation related to the severity of LC and sarcopenia. As immune alterations could worsen with disease progression, it is possible to hypothesize that the impairment contributing to sarcopenia would also worsen at a later stage.

To conclude, utilizing data from 100 patients, this study was the first to examine the role of NETs formation in patients with sarcopenia. There was a tendency toward an increase in spontaneous NETs formation in the sarcopenia group without LC, suggesting a possible association between increased NETs formation and sarcopenia. AI-based algorithms can be

a standardized and efficient way of otherwise laborious analysis of NETs formation by eye, facilitating the development of neutrophil function screening panels in clinical practice and making it feasible to introduce NETs formation analysis for large-scale clinical studies. Hence, this study emphasizes the necessity for more research to fully understand the role of NETs formation in LC and sarcopenia and whether NETs formation becomes a biomarker for sarcopenia.

Literature Cited

1. Cruz-Jentoft AJ, Sayer AA. Sarcopenia. The Lancet 2019; 393(10191):2636–46.

2. Cruz-Jentoft AJ, Bahat G, Bauer J, Boirie Y, Bruyère O, Cederholm T et al. Sarcopenia: revised European consensus on definition and diagnosis. Age Ageing 2019; 48(1):16–31.

3. Rosenberg IH. Sarcopenia: origins and clinical relevance. The Journal of Nutrition 1997; 127(5 Suppl):990S-991S.

4. Cruz-Jentoft AJ, Baeyens JP, Bauer JM, Boirie Y, Cederholm T, Landi F et al. Sarcopenia: European consensus on definition and diagnosis: Report of the European Working Group on Sarcopenia in Older People. Age Ageing 2010; 39(4):412–23.

5. Anker SD, Morley JE, Haehling S von. Welcome to the ICD-10 code for sarcopenia. Journal of Cachexia, Sarcopenia and Muscle 2016; 7(5):512–4.

6. Barazzoni R, Bischoff SC, Boirie Y, Busetto L, Cederholm T, Dicker D et al. Sarcopenic obesity: Time to meet the challenge. Clin Nutr 2018; 37(6 Pt A):1787–93.

7. Wang T. Searching for the link between inflammaging and sarcopenia. Ageing Res Rev 2022; 77:101611.

8. Wilson D, Jackson T, Sapey E, Lord JM. Frailty and sarcopenia: The potential role of an aged immune system. Ageing Res Rev 2017; 36:1–10.

9. Riuzzi F, Sorci G, Arcuri C, Giambanco I, Bellezza I, Minelli A et al. Cellular and molecular mechanisms of sarcopenia: the S100B perspective. Journal of Cachexia, Sarcopenia and Muscle 2018; 9(7):1255–68.

10. Ginès P, Krag A, Abraldes JG, Solà E, Fabrellas N, Kamath PS. Liver cirrhosis. The Lancet 2021; 398(10308):1359–76.

11. Bernsmeier C, van der Merwe S, Périanin A. Innate immune cells in cirrhosis. J Hepatol 2020; 73(1):186–201.

12. Schuppan D, Afdhal NH. Liver cirrhosis. The Lancet 2008; 371(9615):838–51.

13. Sepanlou SG, Safiri S, Bisignano C, Ikuta KS, Merat S, Saberifiroozi M et al. The global, regional, and national burden of cirrhosis by cause in 195 countries and territories,

1990–2017: a systematic analysis for the Global Burden of Disease Study 2017. The Lancet Gastroenterology & Hepatology 2020; 5(3):245–66.

14. Pimpin L, Cortez-Pinto H, Negro F, Corbould E, Lazarus JV, Webber L et al. Burden of liver disease in Europe: Epidemiology and analysis of risk factors to identify prevention policies. J Hepatol 2018; 69(3):718–35.

15. Dasarathy S, Merli M. Sarcopenia from mechanism to diagnosis and treatment in liver disease. J Hepatol 2016; 65(6):1232–44.

16. Tantai X, Liu Y, Yeo YH, Praktiknjo M, Mauro E, Hamaguchi Y et al. Effect of sarcopenia on survival in patients with cirrhosis: A meta-analysis. J Hepatol 2022; 76(3):588–99.

17. Bhanji RA, Montano-Loza AJ, Watt KD. Sarcopenia in Cirrhosis: Looking Beyond the Skeletal Muscle Loss to See the Systemic Disease. Hepatology 2019; 70(6):2193–203.

18. Albillos A, Martin-Mateos R, van der Merwe S, Wiest R, Jalan R, Álvarez-Mon M. Cirrhosis-associated immune dysfunction. Nat Rev Gastroenterol Hepatol 2022; 19(2):112–34.

19. Sapey E, Greenwood H, Walton G, Mann E, Love A, Aaronson N et al. Phosphoinositide 3-kinase inhibition restores neutrophil accuracy in the elderly: toward targeted treatments for immunosenescence. Blood 2014; 123(2):239–48.

20. Papayannopoulos V. Neutrophil extracellular traps in immunity and disease. Nat Rev Immunol 2018; 18(2):134–47.

21. Ley K, Hoffman HM, Kubes P, Cassatella MA, Zychlinsky A, Hedrick CC et al. Neutrophils: New insights and open questions. Science Immunology 2018; 3(30). Available from: URL: http://immunology-1sciencemag-1org-10013b5t304c3.han.medunigraz.at/content/3/30/eaat4579.long.

22. Pérez-Figueroa E, Álvarez-Carrasco P, Ortega E, Maldonado-Bernal C. Neutrophils: Many Ways to Die. Front. Immunol. 2021; 12:631821.

23. Brinkmann V, Reichard U, Goosmann C, Fauler B, Uhlemann Y, Weiss DS et al. Neutrophil extracellular traps kill bacteria. Science 2004; 303(5663):1532–5.

24. Urban CF, Reichard U, Brinkmann V, Zychlinsky A. Neutrophil extracellular traps capture and kill Candida albicans yeast and hyphal forms. Cell Microbiol 2006; 8(4):668–76.

25. Saitoh T, Komano J, Saitoh Y, Misawa T, Takahama M, Kozaki T et al. Neutrophil extracellular traps mediate a host defense response to human immunodeficiency virus-1. Cell Host Microbe 2012; 12(1):109–16.

26. Abi Abdallah DS, Lin C, Ball CJ, King MR, Duhamel GE, Denkers EY. Toxoplasma gondii triggers release of human and mouse neutrophil extracellular traps. Infect Immun 2012; 80(2):768–77.

27. Yousefi S, Mihalache C, Kozlowski E, Schmid I, Simon HU. Viable neutrophils release mitochondrial DNA to form neutrophil extracellular traps. Cell Death Differ 2009; 16(11):1438–44.

28. Yipp BG, Petri B, Salina D, Jenne CN, Scott BNV, Zbytnuik LD et al. Infection-induced NETosis is a dynamic process involving neutrophil multitasking in vivo. Nat Med 2012; 18(9):1386–93.

29. Fuchs TA, Abed U, Goosmann C, Hurwitz R, Schulze I, Wahn V et al. Novel cell death program leads to neutrophil extracellular traps. Journal of Cell Biology 2007; 176(2):231–41.

30. Honda M, Kubes P. Neutrophils and neutrophil extracellular traps in the liver and gastrointestinal system. Nat Rev Gastroenterol Hepatol 2018; 15(4):206–21.

31. Buchanan JT, Simpson AJ, Aziz RK, Liu GY, Kristian SA, Kotb M et al. DNase expression allows the pathogen group A Streptococcus to escape killing in neutrophil extracellular traps. Curr Biol 2006; 16(4):396–400.

32. Buhr N de, Köckritz-Blickwede M von. How Neutrophil Extracellular Traps Become Visible. Journal of Immunology Research 2016; 2016:4604713.

33. Zenlander R, Havervall S, Magnusson M, Engstrand J, Ågren A, Thålin C et al. Neutrophil extracellular traps in patients with liver cirrhosis and hepatocellular carcinoma. Sci Rep 2021; 11(1):18025.

34. Leshner M, Wang S, Lewis C, Zheng H, Chen XA, Santy L et al. PAD4 mediated histone hypercitrullination induces heterochromatin decondensation and chromatin unfolding to form neutrophil extracellular trap-like structures. Front Immunol 2012; 3:307.

35. Yipp BG, Kubes P. NETosis: how vital is it? Blood 2013; 122(16):2784–94.

36. Agraz-Cibrian JM, Segura-Ortega JE, Delgado-Rizo V, Fafutis-Morris M. Alterations in neutrophil extracellular traps is associated with the degree of decompensation of liver cirrhosis. J Infect Dev Ctries 2016; 10(5):512–7.

37. Agraz-Cibrián JM, Delgado-Rizo V, Segura-Ortega JE, Maldonado-Gómez HA, Zambrano-Zaragoza JF, Durán-Avelar MdJ et al. Impaired neutrophil extracellular traps and inflammatory responses in the peritoneal fluid of patients with liver cirrhosis. Scandinavian Journal of Immunology 2018; 88(5):e12714. Available from: URL: https://onlinelibrary-1wiley-1com-10013b5t304c3.han.medunigraz.at/doi/10.1111/sji.12714.

38. Blasi A, Patel VC, Adelmeijer J, Azarian S, Aziz F, Fernández J et al. Plasma levels of circulating DNA are associated with outcome, but not with activation of coagulation in decompensated cirrhosis and ACLF. JHEP Rep 2019; 1(3):179–87.

39. Yang L-Y, Luo Q, Lu L, Zhu W-W, Sun H-T, Wei R et al. Increased neutrophil extracellular traps promote metastasis potential of hepatocellular carcinoma via provoking tumorous inflammatory response. J Hematol Oncol 2020; 13(1):3.

40. van der Windt DJ, Sud V, Zhang H, Varley PR, Goswami J, Yazdani HO et al. Neutrophil extracellular traps promote inflammation and development of hepatocellular carcinoma in nonalcoholic steatohepatitis. Hepatology 2018; 68(4):1347–60.

41. Rebernick R, Fahmy L, Glover C, Bawadekar M, Shim D, Holmes CL et al. DNA Area and NETosis Analysis (DANA): a High-Throughput Method to Quantify Neutrophil Extracellular Traps in Fluorescent Microscope Images. Biol Proced Online 2018; 20(1):7.

42. van Breda SV, Vokalova L, Neugebauer C, Rossi SW, Hahn S, Hasler P. Computational Methodologies for the in vitro and in situ Quantification of Neutrophil Extracellular Traps. Front. Immunol. 2019; 10:1562.

43. Buhr N de, Köckritz-Blickwede M von. Detection, Visualization, and Quantification of Neutrophil Extracellular Traps (NETs) and NET Markers. In: Quinn MT, DeLeo FR,

editors. Neutrophil. New York, NY: Springer US; 2020. p. 425–42 (Methods in Molecular Biology; vol. 2087).

44. Thålin C, Daleskog M, Göransson SP, Schatzberg D, Lasselin J, Laska A-C et al. Validation of an enzyme-linked immunosorbent assay for the quantification of citrullinated histone H3 as a marker for neutrophil extracellular traps in human plasma. Immunol Res 2017; 65(3):706–12.

45. Masuda S, Nakazawa D, Shida H, Miyoshi A, Kusunoki Y, Tomaru U et al. NETosis markers: Quest for specific, objective, and quantitative markers. Clin Chim Acta 2016; 459:89–93.

46. Mohanty T, Sørensen OE, Nordenfelt P. NETQUANT: Automated Quantification of Neutrophil Extracellular Traps. Front. Immunol. 2017; 8:1999.

47. Zhao W, Fogg DK, Kaplan MJ. A novel image-based quantitative method for the characterization of NETosis. Journal of Immunological Methods 2015; 423:104–10.

48. Ginley BG, Emmons T, Lutnick B, Urban CF, Segal BH, Sarder P. Computational detection and quantification of human and mouse neutrophil extracellular traps in flow cytometry and confocal microscopy. Sci Rep 2017; 7(1):17755.

49. Hazeldine J, Harris P, Chapple IL, Grant M, Greenwood H, Livesey A et al. Impaired neutrophil extracellular trap formation: a novel defect in the innate immune system of aged individuals. Aging Cell 2014; 13(4):690–8.

50. Xing Y, Jiang Y, Xing S, Mao T, Guan G, Niu Q et al. Neutrophil extracellular traps are associated with enhanced procoagulant activity in liver cirrhosis patients with portal vein thrombosis. J Clin Lab Anal 2022; 36(5):e24433.

51. Fuchs TA, Brill A, Duerschmied D, Schatzberg D, Monestier M, Myers DD et al. Extracellular DNA traps promote thrombosis. Proc Natl Acad Sci U S A 2010; 107(36):15880–5.

52. Kimball AS, Obi AT, Diaz JA, Henke PK. The Emerging Role of NETs in Venous Thrombosis and Immunothrombosis. Front Immunol 2016; 7:236.

53. Jiménez-Alcázar M, Rangaswamy C, Panda R, Bitterling J, Simsek YJ, Long AT et al. Host DNases prevent vascular occlusion by neutrophil extracellular traps. Science 2017; 358(6367):1202–6.

54. Wigerblad G, Kaplan MJ. Neutrophil extracellular traps in systemic autoimmune and autoinflammatory diseases. Nat Rev Immunol 2023; 23(5):274–88.

55. Khandpur R, Carmona-Rivera C, Vivekanandan-Giri A, Gizinski A, Yalavarthi S, Knight JS et al. NETs are a source of citrullinated autoantigens and stimulate inflammatory responses in rheumatoid arthritis. Sci Transl Med 2013; 5(178):178ra40.

56. Hakkim A, Fürnrohr BG, Amann K, Laube B, Abed UA, Brinkmann V et al. Impairment of neutrophil extracellular trap degradation is associated with lupus nephritis. Proc Natl Acad Sci U S A 2010; 107(21):9813–8.

57. Warnatsch A, Ioannou M, Wang Q, Papayannopoulos V. Inflammation. Neutrophil extracellular traps license macrophages for cytokine production in atherosclerosis. Science 2015; 349(6245):316–20.

58. Brinkmann V. Neutrophil Extracellular Traps in the Second Decade. J Innate Immun 2018; 10(5-6):414–21.

59. Drury B, Hardisty G, Gray RD, Ho G-T. Neutrophil Extracellular Traps in Inflammatory Bowel Disease: Pathogenic Mechanisms and Clinical Translation. Cell Mol Gastroenterol Hepatol 2021; 12(1):321–33.

60. Brill A, Fuchs TA, Savchenko AS, Thomas GM, Martinod K, Meyer SF de et al. Neutrophil extracellular traps promote deep vein thrombosis in mice. J Thromb Haemost 2012; 10(1):136–44.

61. Martinod K, Demers M, Fuchs TA, Wong SL, Brill A, Gallant M et al. Neutrophil histone modification by peptidylarginine deiminase 4 is critical for deep vein thrombosis in mice. Proc Natl Acad Sci U S A 2013; 110(21):8674–9.

62. Mutua V, Gershwin LJ. A Review of Neutrophil Extracellular Traps (NETs) in Disease: Potential Anti-NETs Therapeutics. Clinic Rev Allerg Immunol 2021; 61(2):194–211.